Trench Bending Initiation: Upper Plate Strain Pattern and Volcanism. Insights From the Lesser Antilles Arc, St. Barthelemy Island, French West Indies

Lucie Legendre, Melody Philippon, Philippe Munch, Jean-Len Leticee, Mélanie Noury, G. Maincent, Jean-Jacques Cornee, A. Caravati, Jean-Frederic Lebrun, Yves Mazabraud

Tectonics

RESEARCH ARTICLE
10.1029/2017TC004921

Key Points:
- The extinct Lesser Antilles arc shows a westward migration of the tectono-magmatic activity during the middle Eocene-Miocene period
- Paleostress inversions reveal that the stress regime evolved from pure to radial extension over the Eocene-Lower Miocene time span
- This switch in the upper plate strain pattern accommodates the bending of the trench that followed the Bahamas Bank collision

Correspondence to:
M. Philippon,
melody.philippon@univ-antilles.fr

Citation:
Legendre, L., Philippon, M., Münch, P., Leticée, J. L., Noury, M., Maincent, G., et al. (2018). Trench bending initiation: Upper plate strain pattern and volcanism. Insights from the Lesser Antilles arc, St. Barthelemy Island, French West Indies. *Tectonics*, *37*, 2777–2797. https://doi.org/10.1029/2017TC004921

Received 11 DEC 2017
Accepted 5 JUN 2018
Accepted article online 13 JUN 2018
Published online 4 SEP 2018

Trench Bending Initiation: Upper Plate Strain Pattern and Volcanism. Insights From the Lesser Antilles Arc, St. Barthelemy Island, French West Indies

L. Legendre[1], M. Philippon[1], Ph. Münch[2], J. L. Leticée[1], M. Noury[1], G. Maincent[3], J. J. Cornée[1,2], A. Caravati[1], J. F. Lebrun[1], and Y. Mazabraud[1]

[1]Géosciences Montpellier, UMR5243, CNRS-Université des Antilles-Université de Montpellier, Campus de Fouillole, Pointe-à-Pitre, France, [2]Géosciences Montpellier, UMR5243, CNRS-Université de Montpellier-Université des Antilles, Place Eugène Bataillon, Montpellier, France, [3]Dévé, St. Barthelemy, France

Abstract The upper plate deformation pattern reflects the mechanical behavior of subduction zones. Here we focus on the consequences of the entrance of a buoyant bank into the Caribbean subduction zone during the Eocene by studying the oldest exposed rocks belonging to the Lesser Antilles volcanic arc. Using a novel geochronological data set, we show that the volcanic arc activity on the island of St. Barthelemy spanned over the mid-Eocene to early Miocene with a westward migration of the tectono-volcanic activity, which is comparable to what has already been observed on other volcanic islands in the Lesser Antilles. The kinematics analysis allows us to identify a switch in the stress field from pure to radial extension at the Oligo-Miocene hinge with a subhorizontal σ_3 that has a mean trend of N20°. A three-step restoration of the regional deformation indicates that this switch from pure parallel-to-the-trench extension to radial extension may reflect a strain partitioning initiation affecting the upper Caribbean Plate in response to trench bending that followed the entrance of the Bahamas Bank into the subduction zone. We show that the northern end of the Lesser Antilles arc shows a tectono-volcanic evolution which is similar to the southern one. The north-south dichotomy in the perpendicular-to-the-trench extension, 15% in the north versus 30% in the south, may reflect different slab ends that are highly curved to the north (restraining the extension in the upper plate) versus a tear to the south (allowing a larger amount of extension within the upper plate).

1. Introduction

In subduction zones, the upper plate deformation pattern reflects the dynamics of the downgoing slab. The slab dip controls the location of the volcanic arc (England et al., 2004; Syracuse & Abers, 2006; Tatsumi et al., 1986), whereas interplate coupling (a function of the asperities and fluid circulations at the interface of the plates) as well as trench deformation (i.e., bending, rollback, and advance) are accommodated by upper plate strain, which may be partitioned and may result in the uplift or subsidence of the forearc-arc and back-arc regions (Heuret & Lallemand, 2005; Lallemand, 1999). In this regard, by studying the upper plate deformation pattern of the subduction zones it is possible to picture the evolution of both the geometry and mechanical behavior of the subduction zone through time.

The Lesser Antilles subduction zone trends between the North and South American Plates and is one of the shortest (1,400 km long) highly curved trenches in the world (Westbrook & McCann, 1986). Its morphology is comparable to the poorly known Scotia subduction zone located between South America and Antarctica (Barker, 1970; Lynner & Long, 2013). The peculiar curvature of the Lesser Antilles trench has been acquired since the Paleocene subsequent to the entrance of the buoyant Bahamas Bank in the Greater Antilles subduction zone. This event locked the subduction process, triggering the plate boundary reorganization, cessation, and migration of the arc in the forearc of the subduction zone together with upper plate deformation (Mann, 1999; Pindell & Barrett, 1990; Westercamp & Andreieff, 1983b).

However, there is scant information about the processes that occurred in the northern Lesser Antilles following the entrance of the Bahamas Bank in the subduction zone, either in terms of arc initiation in the forearc area of the subduction zone or in terms of the stress regime accompanying this initiation. In this paper, our aim is to provide new constraints on the tectono-magmatic evolution of the Lesser Antilles volcanic arc. We identify the Eocene-Oligocene interval as a key period to study the initiation of the Lesser Antilles arc

magmatism and are focusing on St. Barthelemy Island as it is known to display middle Eocene limestones and middle Eocene to early Oligocene volcanoclastic and magmatic rocks. We propose a revised chronology of the magmatism based on novel geochronological data. These new ages, coupled with a high-resolution structural and kinematic analysis of both brittle and ductile deformations, can be used to characterize the evolution of the stress field through time from the middle Eocene to the early Miocene. Our data set allows to discuss the tectono-magmatic evolution of the island over this time interval corresponding to the birth and development of the Lesser Antilles volcanic arc. This evolution is discussed within the framework of the geodynamical evolution of the Caribbean subduction zone.

2. Geological Context

2.1. Regional Geodynamical Evolution

Since the Hauterivian interval (134–131 Ma), the North and South American Plates are subducted below the north-northeastern boundary of the Caribbean Plate along the Greater Arc of the Caribbean (GAC) subduction zone (Pindell et al., 2012; Figure 1a). In the northern Lesser Antilles, the GAC-related late Cretaceous-Paleocene arc magmatism was exposed on the island of St. Croix (Virgin Islands) from approximately 74 to 64 Ma (Speed et al., 1979). To the south, this arc was exposed on the Aves Ridge between approximately 88 and 59 Ma (Bouysse et al., 1985; Fox et al., 1971; Neill et al., 2011; Figure 1a). There is no evidence for late Cretaceous-Paleocene magmatism east of the Aves Ridge, that is, on the Lesser Antilles islands (Figure 1b).

During the early Eocene, the collision of the buoyant Bahamas Bank with the Caribbean Plate triggered a decrease in the subduction rate (Ladd & Sheridan, 1987; Pindell & Kennan, 2001, 2009; Uchupi et al., 1971; Figure 1a). Since then, to the north, the eastward extrusion of the Caribbean Plate is accommodated by a large-scale sinistral strike-slip fault. The arc magmatism resumed during the middle Eocene. Evidence for a middle Eocene arc is scarce and is mainly located on the Anguilla Bank in the northeastern Lesser Antilles arc (Figure 1b). The oldest magmatic episode known on St. Barthelemy is middle Eocene in age and consists of submarine volcanism and slightly younger intrusions of tholeiitic and calc-alkaline affinities, respectively. On the neighboring island of St. Martin, an early-to-middle Eocene mixed volcanoclastic-carbonate series, affected by low-grade metamorphism, extensively crops out (Andreieff et al., 1987; Bonneton & Vila, 1983; Christman, 1953). On the island of Antigua, southeast of St. Barthelemy, a basaltic lava yielded a minimum whole rock K/Ar age at approximately 40 Ma (Briden et al., 1979; Nagle et al., 1976); however, due to weathering, this age needs to be considered very cautiously. West of St. Barthelemy, there is no evidence for middle Eocene volcanic activity on either the Saba Bank (Church & Allison, 2005) or on St. Croix (Speed et al., 1979) despite their position in the prolongation of the Aves Ridge (Figure 1b). These observations are consistent with the waning of the Cretaceous-Paleocene GAC located on the Aves Ridge. Thus, following the entrance of the Bahamas Bank into the subduction zone, the volcanism shifted eastward in the forearc basin of the GAC.

During the early Oligocene, the GAC subduction zone was progressively sutured from west to east at its northern edge (i.e., along Cuba). East of the suture, the plate boundary was a sinistral strike-slip (Hispaniola) whereas further east (Puerto Rico and eastward), subduction was still ongoing and rolling back eastward (white arrow, Figure 1a). Contemporaneously, the upper Caribbean Plate itself was affected by a large-scale strike-slip fault, which has been accommodating the opening of the Cayman Trough since 49 Ma (Mann, 2012).

Since the late Oligocene, the eastward retreat of the trench and its progressive bending have both been accommodated by the eastward propagation of this sinistral strike-slip fault in the upper plate, reaching the eastern tip of Puerto Rico (Escalona & Mann, 2010; Pindell & Kennan, 2001, 2009). This was responsible for (i) the opening of the Mona rift west of the Puerto Rico-Virgin Islands block (PRVI block), triggering its 25° counterclockwise rotation and (ii) to the east of it, the opening of the Anegada Trough, a major NE-SW trending pull-apart basin separating the PRVI block from the Lesser Antilles and St. Croix (Jansma et al., 2000; Jany et al., 1990; Mann et al., 2005; Reid et al., 1991) (Figure 1). The Oligocene magmatism occurred mainly on the islands of St. Martin and Antigua but west of St. Barthelemy and north of the Saba Bank; volcanic clasts from the Arcante 3 dredge 119D yielded Oligocene ages (approximately 29 to 24 Ma; Bouysse et al., 1985) indicating that volcanic activity also occurred in this area (Figure 1b). On St. Martin, two large magmatic bodies intruding the Eocene volcano-sedimentary series yielded K/Ar ages (whole rock as well as hornblende and biotite) between approximately 31 and 28 Ma (Briden et al., 1979; Nagle et al., 1976).

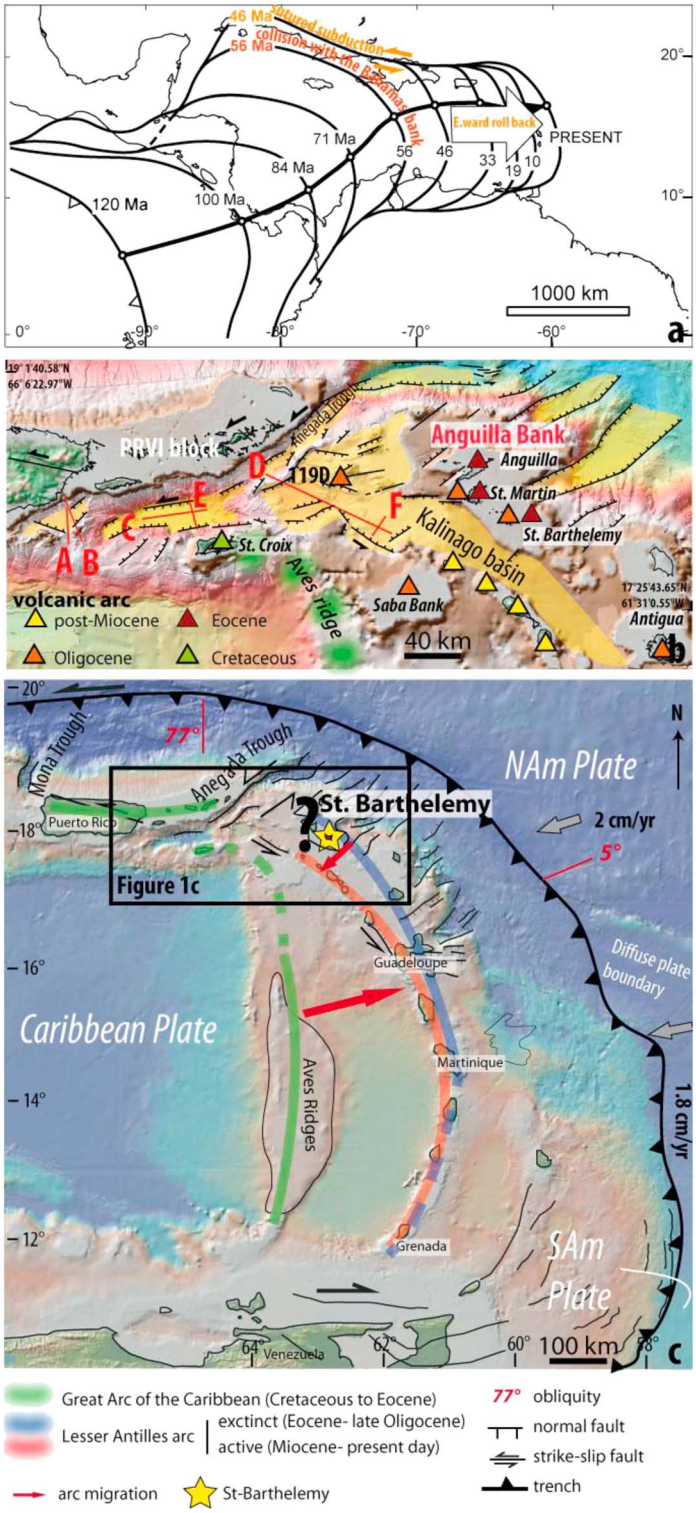

Figure 1. (a) Geodynamical evolution of the northeastern Caribbean Plate boundary after Pindell and Kennan (2009). (b) Regional synthetic map of the northern Lesser Antilles showing the volcanic rock occurrences, their ages, and the main faults. The red lines and letters indicate the seismic lines we restored in section 5.2. (c) Structural map of the Lesser Antilles subduction zone after Feuillet et al. (2002, 2010) and Laurencin et al. (2017). The gray arrows indicate the convergence rates (DeMets et al., 2000). The yellow star indicates the location of St. Barthelemy Island. The terms NAm and SAm plates refer to the North and South American Plates, respectively. The green, blue, and red lines show the Greater arc of the Caribbean, the extinct Lesser Antilles arc, and the present-day Lesser Antilles arc, respectively. PRVI = Puerto Rico-Virgin Islands.

Calc-alkaline volcanic intercalations were recognized in St. Martin within the Eocene volcano-sedimentary series but the whole rock K/Ar dating of the volcanic rocks yielded ages between approximately 31 and 26 Ma (Briden et al., 1979), which is not consistent with the biostratigraphic ages (Andreieff et al., 1987). This suggests that these volcanic rocks should be considered as near-surface sills that are also related to an Oligocene magmatic episode. On Antigua, the available whole rock K/Ar dating mainly points to the late Oligocene-early Miocene period (approximately 24 to 20 Ma); however, these are solely minimum ages; in addition, because of the severe weathering of the samples, these ages must be considered with caution (Briden et al., 1979; Nagle et al., 1976; Figure 1b). This volcanic arc extended southward in Martinique where it also migrated westward through time (Andreieff et al., 1987). The oldest volcanic units (Basal Complex and St. Anne Series) on this island were recently dated again between approximately 25 and 21 Ma, that is, late Oligocene-early Miocene (Germa et al., 2011).

Since the late Oligocene-early Miocene, the volcanic arc of the Lesser Antilles shows a peculiar feature; south of Martinique, the volcanic activity was continuous and slightly migrated westward (less than 10 km, i.e., the width of the island) whereas north of this island, it ceased during the late Oligocene-early Miocene interval and migrated westward to its present-day location (Figure 1c). The duration of the volcanic hiatus is estimated to be approximately 10 Myr (i.e., 30 to 20 Ma according to Bouysses & Westercamp, 1990). Therefore, presently, remnants of the Eocene-Oligocene arc (i.e., the islands of St. Martin, St. Barthelemy, and Antigua) stand in the forearc of the early Miocene-present-day volcanic arc (Bouysse et al., 1990; Pindell & Kennan, 2001, 2009).

The present-day morphology of the Lesser Antilles subduction zone results from this latter 56-Ma geodynamical evolution. The subduction of the North and South American Plates is oriented WSW. As the trench is convex, its obliquity increases from a minimum value of 5° at the latitude of Guadeloupe to an obliquity of 77° at the latitude of the Anegada Trough and to nearly pure strike-slip offshore western Hispaniola (Figure 1c). Oblique subduction is accommodated by strain partitioning in the Caribbean Plate, which shows a large-scale sinistral strike-slip fault along the Greater Antilles, and the Anegada Trough sinistral strike-slip system links up with the Lesser Antilles (DeMets et al., 2000; Deng & Sykes, 1995; Feuillet et al., 2001; Laurencin et al., 2017; Stein et al., 1982). Along the northern Lesser Antilles, the strain partitioning is accommodated by parallel-to-the-trench en echelon faults along the arc and perpendicular-to-the-trench grabens in the forearc (Figure 1b; Feuillet et al., 2002, 2010, 2011; Lopez et al., 2006; Manaker et al., 2008). However, this interpretation is challenged by the following observations along the Lesser Antilles subduction zone: (i) the low degree of subduction obliquity ($<5°$) from the northern Lesser Antilles islands southward, (ii) the very limited occurrence of strike-slip focal mechanisms (Gonzàlez et al., 2017; Stein et al., 1982), (iii) indications for low coupling at the subduction interface (Symithe et al., 2015), and (iv) evidence showing that, perpendicular to the trench, the grabens are not neoformed but localized above inherited structures (Corsini et al., 2011; De Min et al., 2015; Lardeaux et al., 2013; Münch et al., 2014).

2.2. Geology of St. Barthelemy

St. Barthelemy belongs to the Anguilla Bank, a shallow Miocene to Holocene reefal platform from which two other islands emerge: Anguilla and St. Martin (Christman, 1953) (Figure 1b). The bank delimits the northernmost tip of the Lesser Antilles remnants of the Eo-Oligocene volcanic arc and is bounded (i) to the northwest by a series of basins trending parallel to the Anegada Trough, (ii) to the west by the 800-m-deep Kalinago Basin, and (iii) to the east by the outer forearc (Figure 1c). The island of St. Barthelemy consists of middle Eocene volcaniclastic and limestone deposits interbedded with submarine lava flows and the whole series is intruded by late Eocene to Oligocene magmatic intrusions (Westercamp & Andreieff, 1983b; Figure 2).

The sedimentary record displays six sedimentary units, deposited during periods of relative volcanic quiescence. The two lowest units are comprised of a carbonate platform deposited in littoral conditions. The overlaying four carbonate platform units were deposited in a more distal depositional setting (Andreieff et al., 1987; Westercamp & Andreieff, 1983b). The two lowest units were dated as middle Eocene in age (Lutetian to early Bartonian) on the basis of the occurrence of the benthic foraminifer *Polylepidina antillea*, which points to the P11 and P12 planktonic foraminifera biozones (Andreieff et al., 1987; Westercamp & Andreieff, 1983b). The four upper units were also dated as belonging to the middle Eocene (late Lutetian to early Bartonian) on the basis of the cooccurrence of the benthic foraminifera *P. antillea* and *Nummulites striatoreticulus*, which points to the P12 biozone (Figure 2).

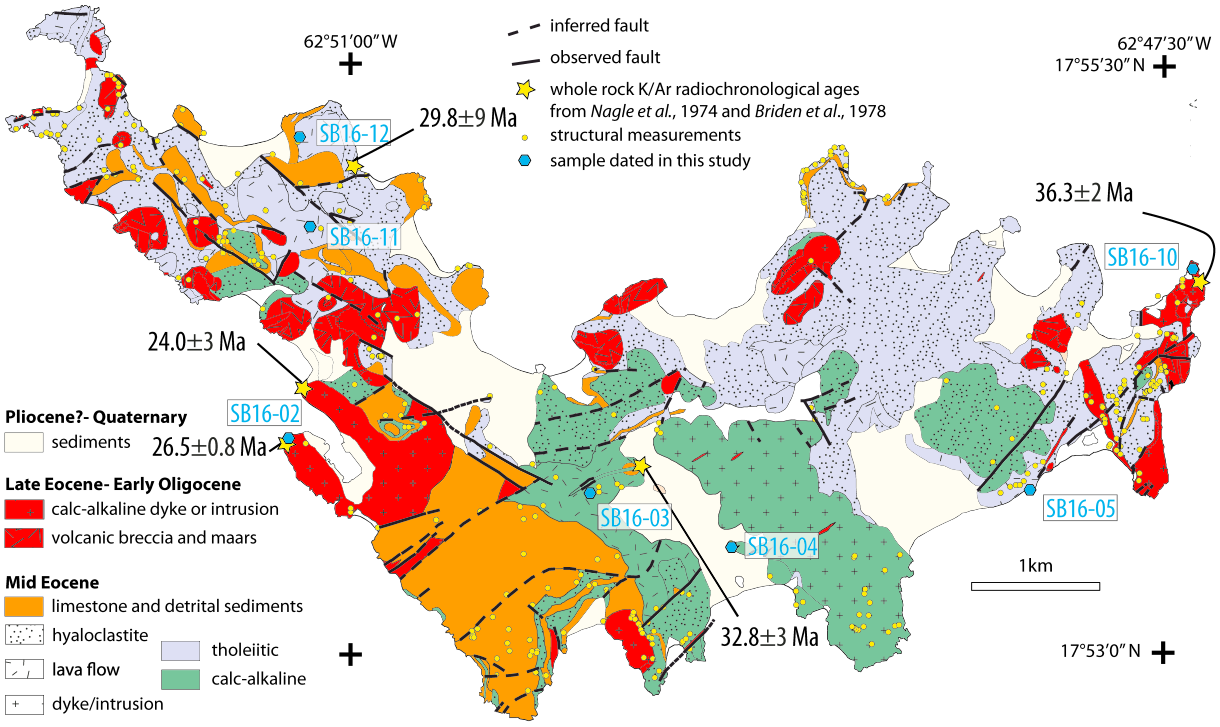

Figure 2. Simplified geological map of St. Barthelemy showing the main lithologies and geochemical affinities of magmatic rocks (modified after De Reynal de Saint-Michel, 1966, and Westercamp & Andreieff, 1983a).

Three magmatic episodes have been previously distinguished (Westercamp & Andreieff, 1983a, 1983b; Figure 2). The two oldest episodes were not dated but were considered as coeval with the deposition of the carbonate platform; therefore, they most likely occurred during middle Eocene times (late Lutetian-early Bartonian), during approximately ~3.4 Myr between 43.88 and 40.49 Ma (calibrated age for the biozones following Vandenberghe et al., 2012). However, it must be pointed out that (i) the geometrical relationships between the carbonate platform deposits and magmatic formations as depicted on the geological map (Westercamp & Andreieff, 1983a) are sometimes debatable, and (ii) a whole rock K/Ar age obtained on an andesitic flow, mapped below one of the four latest carbonate platforms at 29.8 ± 9 Ma (Briden et al., 1979; Nagle et al., 1976) was rejected because it was not concordant with the biostratigraphic data. The oldest middle Eocene magmatic episode corresponds to a tholeiitic episode and was described mainly in the islets north of St. Barthelemy and in the northern part of St. Barthelemy Island. The second episode, still middle Eocene in age is of calc-alkaline affinity and mainly outcrops in the southeastern part of St. Barthelemy. According to Westercamp and Andreieff (1983a, 1983b), these two magmatic episodes should have occurred along roughly parallel WNW-ESE trends with the older tholeiitic episode north of the younger calc-alkaline one. This southward migration together with this magmatic evolution were both interpreted as resulting from a south-dipping subduction and therefore the magmatism in St. Barthelemy was thought to belong to the GAC (Westercamp & Andreieff, 1983b). The last magmatic episode has a calc-alkaline affinity and cross-cuts all previous sedimentary and magmatic rocks. This episode is characterized by the emplacement of volcanic pipes, with associated breccia and maars, and by two large intrusions (Westercamp & Andreieff, 1983a, 1983b). The previous whole rock K/Ar dating of these intrusions yielded ages ranging from 36.3 ± 2 to 24 ± 3 Ma (Briden et al., 1979; Nagle et al., 1976; Figure 2). According to Westercamp and Andreieff (1983a, 1983b), these intrusions are organized along two main NW-SE trending magmatic centers located at both tips of St. Barthelemy Island. Given that they were considered as synchronous with the magmatism occurring in the neighboring island of St. Martin (Nagle et al., 1976), they were interpreted as representing the onset of the Lesser Antilles arc in the forearc of the GAC.

From a structural point of view, two main directions of faults trending WNW-ESE and NE-SW are shaping the island and have been recognized at the island scale (Christman, 1953; Westercamp & Andreieff, 1983a, 1983b). The proposed distribution of the volcanic centers along two main WNW-ESE middle Eocene

magmatic fronts may suggest a tectonic control on the localization of the magmatism and on the roughly southward migration of the magmatism (Westercamp & Andreieff, 1983b). The carbonate platforms and volcanoclastic deposits are tilted by <20° toward the S-SW. This is consistent with the southward regional tilt, which has been proposed to have occurred prior to the last magmatic event (Westercamp & Andreieff, 1983b). The proposed distribution of the late Eocene-Oligocene intrusions along a NW-SE direction and the occurrence of few NE-SW trending dykes may also suggest a tectonic control on the latest magmatic event (Westercamp & Andreieff, 1983b).

3. Data and Methods

3.1. $^{40}Ar/^{39}Ar$ Dating

The samples were crushed and sieved, and a 100- to 200-μm grain size was retained for feldspar and groundmass separation. After magnetic separation, the plagioclase and groundmass grains were selected under a binocular microscope. The grains were leached with HNO_3 (1 N) for a few minutes and then repeatedly cleaned ultrasonically in distilled water and alcohol. The samples were packed in aluminum foil for irradiation in the core of the Triga Mark II nuclear reactor of Pavia (Italy) with several aliquots of the Taylor Creek sanidine standard (28.619 ± 0.034 Ma in Renne et al., 2010) as a flux monitor. The argon isotopic interferences on K and Ca were determined by the irradiation of KF and CaF_2 pure salts from which the following correction factors were obtained: ($^{40}Ar/^{39}Ar$) K = 0.00969 ± 0.00038, ($^{38}Ar/^{39}Ar$) K = 0.01297 ± 0.00045, ($^{39}Ar/^{37}Ar$) Ca = 0.0007474 ± 0.000021, and ($^{36}Ar/^{37}Ar$) Ca = 0.000288 ± 0.000016. $^{40}Ar/^{39}Ar$ step heating analyses were performed at Géosciences Montpellier (France). The gas extraction and purification lines consist of (a) an IR-CO_2 laser of 100 kHz used at 3–20% power to heat the samples during 60 s, (b) a lens system for beam focusing, (c) a steel chamber, maintained at 10^{-8}–10^{-9} bar, with a copper holder in which 2-mm-diameter blind holes were milled, and (d) two Zr-Al getters for the purification of the gases. The argon isotopes were analyzed with a multicollector mass spectrometer (Argus VI from Thermo-Fisher). The mass discrimination was monitored daily using an automated air pipette and provided a mean value of 0.99985 ± 0.00274 per dalton. Small populations of plagioclase or groundmass were distributed two to three grains deep in the holes of the copper holder and were step-heated. Blank analyses were performed every three sample analyses. The raw data of each step and blank were processed, and the ages were calculated using the ArArCALC software (Koppers, 2002). The criteria for defining plateau ages are as follows: (1) Plateau steps should contain at least 50% released ^{39}Ar, (2) there should be at least three successive steps in the plateau, and (3) the integrated age of the plateau should agree with each apparent age of the plateau within a 2σ confidence interval. All of the subsequent quote uncertainties are at the 2σ level, including the error on the irradiation factor *J*.

3.2. Structural and Kinematics Analysis

This study presents a structural data set consisting of ~1,300 measurements of bedding, fractures, faults, schistosity, and kinematics criteria, acquired over 345 sites across the island during three fieldwork campaigns in order to characterize the kinematics of the brittle deformation affecting St. Barthelemy and its chronology (the structural measurement as well as sampling sites are indicated on Figure 2). We refined the map of St. Barthelemy provided by Westercamp and Andreieff (1983a; Figure 2), remapping geological units, dykes, intrusions and faults, and propose a synthetic W-E cross section of the whole island (Figure 3).

3.3. Paleostress Tensors

We used the right dihedron method to inverse the fault kinematics and obtain the paleostress tensor using WinTensor software (Angelier, 1979; Angelier & Mechler, 1977; Delvaux & Sperner, 2003). WinTensor allows the rotational optimization of the obtained tensor by performing iterative tests on the tensors in order to minimize a misfit function (Delvaux & Sperner, 2003). We performed these inversions with a set of data consisting of the fault strike, dip, plunge of the striae and kinematics criteria. For consistency, a minimum of four structural measurements (fault direction and dip, pitch, and kinematics) is needed to obtain a robust paleotensor. The quality of the inversion is given by QRw (world stress map quality criteria) ranging from A (very good) to E (very bad) depending on the amount of data used for the inversion (n), the ratio between the amount of data used for the inversion, and the amount of input data (n/nt), the deviation between the observed and theoretical slip direction (α_w), the sense of slip confidence level (Cl_w), and the type of structure (fault, fracture, and shear zone). The tensor quality is given by QRt, ranging from A (very good) to E (very bad)

and depends on QRw and on the dispersion of the measured structures: When the data are more highly dispersed, the quality is better (Delvaux & Sperner, 2003).

4. Revision of the Tectono-Magmatic Evolution of St. Barthelemy

4.1. Chronology of the Magmatic Events

The samples were collected at the locations corresponding to the three previously identified magmatic episodes (see the location in Figure 2). The oldest tholeiitic magmatic episode cropping out below the Lutetian carbonate platform, together with the slightly younger calc-alkaline episode (also thought to be Lutetian), has been dated in three and two localities, respectively. We also dated the two late Eocene-Oligocene calc-alkaline main intrusions that correspond to the previously proposed final magmatic episodes. We present our results in Table 1 and Figure 3 following the chronology presented in the available geological map (Westercamp & Andreieff, 1983a).

4.1.1. Oldest Tholeitic and Calc-Alkaline Magmatic Episodes

In the northwestern part of St. Barthelemy Island, basaltic andesite lava flows are widely exposed (Figure 2). According to Westercamp and Andreieff (1983a, 1983b) they should correspond to the oldest volcanics of the island. In this area, we dated groundmass populations (10 mg per experiment) from two different flows: SB16-11 and SB16-12. The available mapping indicates that the southern population, SB16-11, is in a higher stratigraphic position than the northern one SB16-12 (Westercamp & Andreieff, 1983a, 1983b). For sample SB16-12, we performed duplicate analyses that each yielded a saddle-shaped spectrum (Figure 4), indicating an excess of argon, with a mini-plateau age (i.e., $<$50% of the ^{39}Ar released) of 24.56 ± 0.56 Ma and 23.41 ± 0.88 Ma for the central part of the spectra, corresponding to the maximum ages and to 45.4% and 43.9% of the ^{39}Ar released, respectively. The inverse isochron calculations for the steps corresponding to the mini-plateaus yielded concordant ages of 24.25 ± 1.22 Ma (mean square weighted deviation: MSWD = 1.83; initial ^{40}Ar/^{36}Ar ratio of 297.9 ± 7.7) and 23.20 ± 1.36 Ma (MSWD = 2.23; initial ^{40}Ar/^{36}Ar ratio of 296.7 ± 7.1), respectively. The combination of the duplicate analyses yielded a maximum age of 24.12 ± 0.57 Ma corresponding to 43.9% of the ^{39}Ar released and an inverse isochron age of 24.08 ± 1.05 Ma with MSWD = 2.53 and an initial ^{40}Ar/^{36}Ar ratio of 295.9 ± 5.7, indicating that the trapped ^{40}Ar/^{36}Ar is indistinguishable from atmospheric ^{40}Ar/^{36}Ar. The maximum age of 24.12 ± 0.57 Ma for the combined analyses is retained as the best estimate for sample SB16-12. Sample SB16-11 yielded a plateau age of 23.90 ± 3.52 Ma, corresponding to 91.95% of the ^{39}Ar released, and an inverse isochron age of 23.08 ± 4.62 Ma with MSWD = 0.98 for an initial ^{40}Ar/^{36}Ar ratio of 295.8 ± 1.6, indicating that the trapped ^{40}Ar/^{36}Ar is indistinguishable from atmospheric ^{40}Ar/^{36}Ar. The high error on the age is related to the huge abundance of trapped atmospheric argon degassing until the fused step and may be related to the alteration.

The eastern part of St. Barthelemy Island exhibits a relatively continuous section of the base of the series (Figure 3, cross-section AB) comprised of interbedded limestone and volcanoclastic deposits (hyaloclastites) transected by two sets of normal faults (N50° and N140°). On the northern coast, the basal carbonate platform deposits and surrounding hyaloclastites exhibit a bedding trending N80°E with a 5° to 10° southward dip (Figure 3, cross-section AB). To the south of this section, the bedding evolves toward N180°, 10–15°E and a submarine flow of tholeiitic basaltic andesite is interbedded within the hyaloclastites of the upper part of the section and was sampled for dating (SB16-05, Figure 3). We performed duplicate analyses on the plagioclase populations (10 mg each), which each yielded a saddle-shaped spectrum, indicating an excess of argon with a mean age of 44.87 ± 1.73 Ma for the central part of the spectrum (experiment A) and a plateau age of 40.92 ± 2.29 Ma (experiment B) for the central part of spectra, corresponding to 74% and 53.2% of the ^{39}Ar released, respectively. The inverse isochron calculation yielded concordant ages of 43.46 ± 2.08 Ma (experiment A; MSWD = 3.04, initial ^{40}Ar/^{36}Ar ratio of 303.6 ± 7.9) and 38.38 ± 5.15 Ma (experiment B; MSWD = 1.74, initial ^{40}Ar/^{36}Ar ratio of 314 ± 33.3) for the same steps. The initial ^{40}Ar/^{36}Ar ratios indicate that the trapped ^{40}Ar/^{36}Ar is indistinguishable from the atmospheric ^{40}Ar/^{36}Ar. The combination of duplicate analyses yielded a mean age of 43.96 ± 1.49 Ma corresponding to 62.09% of the ^{39}Ar released and an inverse isochron age of 42.82 ± 2.13 Ma with MSWD = 3.38 and an initial ^{40}Ar/^{36}Ar ratio of 300 ± 9.7 (Figure 4). The plateau age of 40.92 ± 2.29 Ma (experiment B) is retained as the best estimate.

In the southeastern and central parts of the island, the mixed volcanic-sedimentary series is crosscut and unconformably overlain by a large calc-alkaline latitic lava-dome (sample SB16-04) and dacitic lava flows

Table 1
$^{40}Ar/^{39}Ar$ Analyses Results

Sample #	Exp.	Longitude	Latitude	Lithology	Material dated	Plateau age (Ma)	±2σ	% 39Ar released	MSWD	Inverse isochrone age (Ma)	±2σ	40Ar/36Ar intercept	±2σ	MSWD	Total fusion age (Ma)	±2σ
SB16-05	A	−62.83163056	17.89460833	Andesitic lava flow	plg	44.87*	1.73	74	4.01	43.46	2.08	303.6	7.9	3.04	48.11	0.86
	B					40.92	2.29	53.19	1.8	38.38	5.15	314	33.3	1.74	43.84	1.3
	A + B combined					43.96*	1.49	62.09	3.71	42.82	2.13	300	9.7	3.38	45.87	0,81
SB16-10		−62.7897073	17.9094932	Andesitic lava dome-flow	plg	39.79	0.78	97.85	1.25	40.32	1.23	294.1	2.2	1.46	39.73	0.89
SB16-04		−62.82213889	17.89054722	Latite lava flow	plg										36.40	0.89
SB16-03		−62.83163056	17.89460833	Dacitic lava flow	groundmass	33.45	1.72	96.36	0.48	33.96	3.19	294.8	3.5	0.56	27.78	4
SB16-02	A	−62.85267778	17.89771389	Quartzic microdiorite	plg	30.13	0.34	100	1.15	29.69	0.53	2974	1.9	1.19	30.34	0.41
	B					30.02	0.34	71.98	0.62	28.75	1.4	309.8	15.3	0.13	30.91	0.37
	A + B combined					30.08	0.26	85.51	0.98	29.79	0.35	297.3	1.5	0.98	30.54	0.29
SB16-12	A	−62.85325	17.91936111	Andesitic lava flow	groundmass	24.56**	0.56	45.39	1.52	24.25	1.22	297.9	7.7	1.83	28.77	0.5
	B	−62.85325	17.91936111			23.41**	0.88	48.87	1.91	23.20	1.64	296.7	7.1	2.23	29.16	0.65
	A + B combined	−62.85325	17.91936111			24.12 **	0.57	43.92	2.23	24.08	1.05	295.9	5.7	2.53	28.98	0.43
SB16-11		−62.85159167	17.91315278	Andesitic lava flow	groundmass	23.90	3.52	91.95	0.73	23.08	4.62	295.8	1.6	0.98	8.80	7.34

Note. The analytical procedure is described in the text. MSWD = mean square weighted deviation; plg = plagioclase; * = mean age; ** = "mini-plateau," that is, with less than 50% of the ^{39}Ar released.

(sample SB16-03) that are associated with hyaloclastites (Figure 3, cross-section BC). Due to extensive alteration, we could only separate twenty clear and unaltered plagioclase grains from sample SB16-04. We fused them in one step after a low-temperature predegassing step in order to remove the atmospheric argon adsorbed on the surface of the grains. This experiment yielded a total fusion age of 36.40 ± 0.89 Ma (Table 1). The groundmass of sample SB16-03 yielded a plateau age of 33.45 ± 1.72 Ma corresponding to 96.36% of the ^{39}Ar released. The inverse isochron calculation yielded an identical age of 33.96 ± 3.19 Ma (MSWD = 0.56) with an initial $^{40}Ar/^{36}Ar$ ratio of 294.8 ± 3.5 that is indistinguishable from the atmospheric ratio (Figure 4). The relatively high errors (~5%) on the ages are related to the abundance of the trapped atmospheric argon that is highly degassed until the fused step and which may be related to weathering. The plateau age of 33.45 ± 1.72 Ma is retained as the best estimate.

4.1.2. Final Calc-Alkaline Magmatic Episode

At the easternmost tip of the island, an andesitic intrusion that was believed to correspond to the last magmatic episode sampled (sample SB16-10, Figure 3 and Table 1). A plagioclase population yielded a plateau age of 39.79 ± 0.78 Ma corresponding to 97.85% of the ^{39}Ar released. The inverse isochron calculation yielded an identical age of 40.32 ± 1.25 Ma (MSWD = 1.46) with an initial $^{40}Ar/^{36}Ar$ ratio of 294.1 ± 2.2 that is indistinguishable from the atmospheric ratio. The plateau age of 39.79 ± 0.78 Ma is retained as the best estimate (Figure 4).

In the central part of the island the large quartz microdiorite intrusion (sample SB16-02, Figure 3 and Table 1) yielded duplicate plateau ages of 30.13 ± 0.34 Ma and 30.02 ± 0.34 Ma, corresponding to 100% and 71.9% of the ^{39}Ar released, respectively. The inverse isochron calculations for the plateau steps yielded concordant ages of 29.69 ± 0.53 Ma (MSWD = 1.19; initial $^{40}Ar/^{36}Ar$ ratio of 297.4 ± 1.9) and 28.75 ± 1.4 Ma (MSWD = 0.13; initial $^{40}Ar/^{36}Ar$ ratio of 309.8 ± 15.3), respectively. The combination of the duplicate analyses yielded a plateau age of 30.08 ± 0.26 Ma corresponding to 85.51% of the ^{39}Ar released and an inverse isochron age of 29.79 ± 0.35 Ma with MSWD = 0.98 and an initial $^{40}Ar/^{36}Ar$ ratio of 297.3 ± 1.5, indicating that the trapped $^{40}Ar/^{36}Ar$ is indistinguishable from the atmospheric $^{40}Ar/^{36}Ar$. The plateau age of combined analyses, that is, 30.08 ± 0.26 Ma, is retained as the best estimate (Figure 4).

4.1.3. Revised Chronostratigraphy

In the eastern part of the island, the new $^{40}Ar/^{39}Ar$ ages for the andesitic (sample SB16-05) and latitic lava flows (sample SB16-04) are consistent with the previously proposed stratigraphy (Westercamp & Andreieff, 1983a, 1983b; Figure 3; section AC, Figure 3). However, the $^{40}Ar/^{39}Ar$ age of 39.79 ± 0.78 Ma for the andesitic intrusion (sample SB16-10), located at the easternmost tip of the island, invalidates the previously proposed age (Westercamp & Andreieff, 1983a, 1983b). This age corresponds to the oldest, middle Eocene, magmatic event and not to the youngest late Eocene-Oligocene one. This result questions the proposed late Eocene-Oligocene age for the small volcanic pipes and associated breccias occurring in the eastern part of the island (light pink, Figure 3).

In the central part of the island, the two new $^{40}Ar/^{39}Ar$ ages also invalidate the previously proposed middle Eocene age for this magmatism (Westercamp & Andreieff, 1983a, 1983b). The latitic and dacitic lava flows yielded ages of 36.40 ± 0.89 Ma (sample SB16-04) and 33.45 ± 1.72 (sample SB16-03), respectively. Therefore, this volcanism is latest Eocene-early Oligocene in age and can no longer be associated with the middle Eocene magmatic event.

To the west of the island, the two dated andesitic lava flows yielded late Oligocene ages (sample SB16-11: 24.31 ± 1.22 Ma and sample SB16-12: 23.92 ± 3.52 Ma), which contradicts the previously proposed middle Eocene age for this volcanism (Westercamp & Andreieff, 1983a, 1983b). It must be pointed out that these new results are concordant with the whole rock K/Ar age (29.8 ± 9 Ma determined by Nagle et al., 1976, and Briden

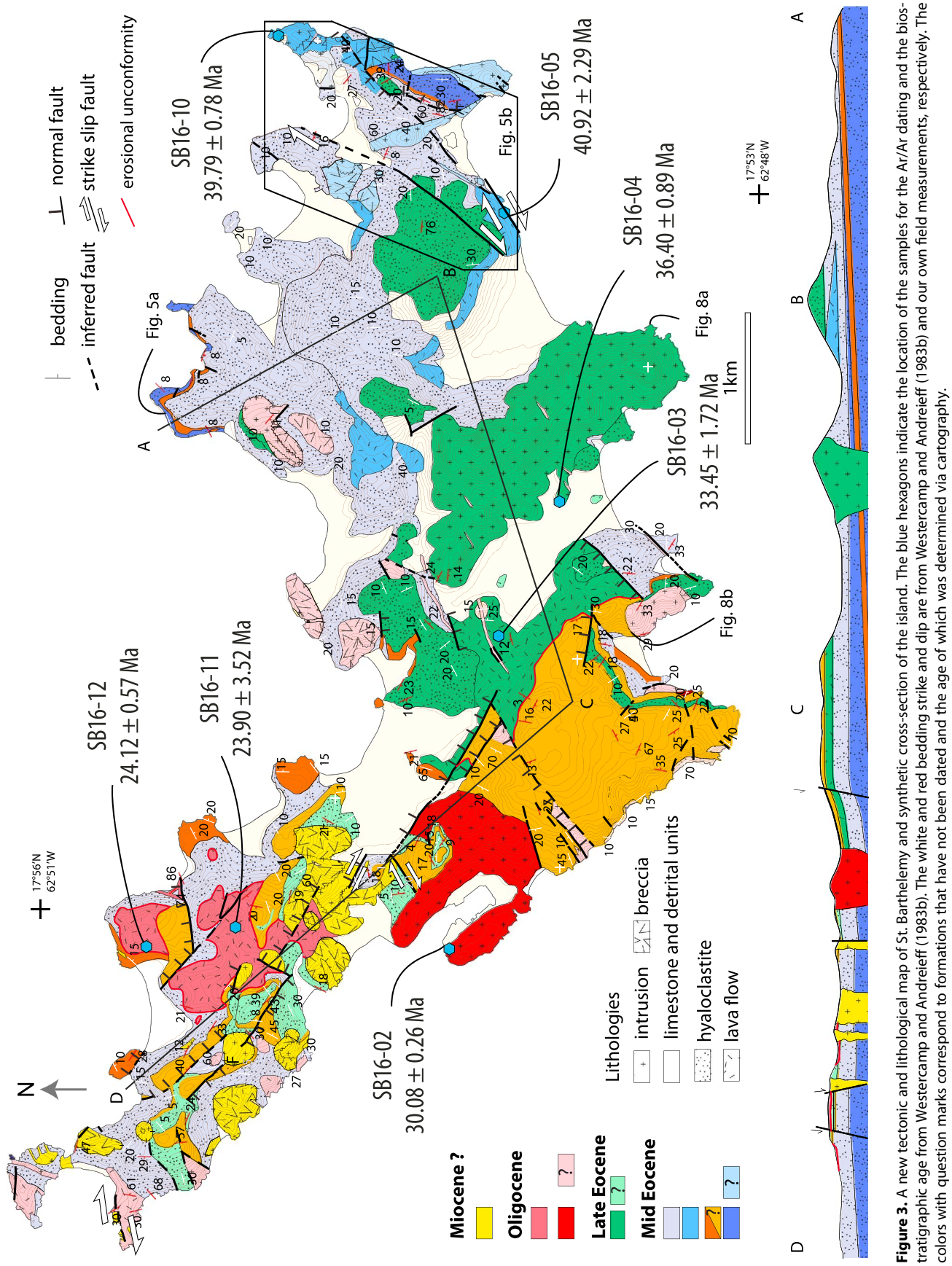

Figure 3. A new tectonic and lithological map of St. Barthelemy and synthetic cross-section of the island. The blue hexagons indicate the location of the samples for the Ar/Ar dating and the biostratigraphic age from Westercamp and Andreieff (1983b). The white and red bedding strike and dip are from Westercamp and Andreieff (1983b) and our own field measurements, respectively. The colors with question marks correspond to formations that have not been dated and the age of which was determined via cartography.

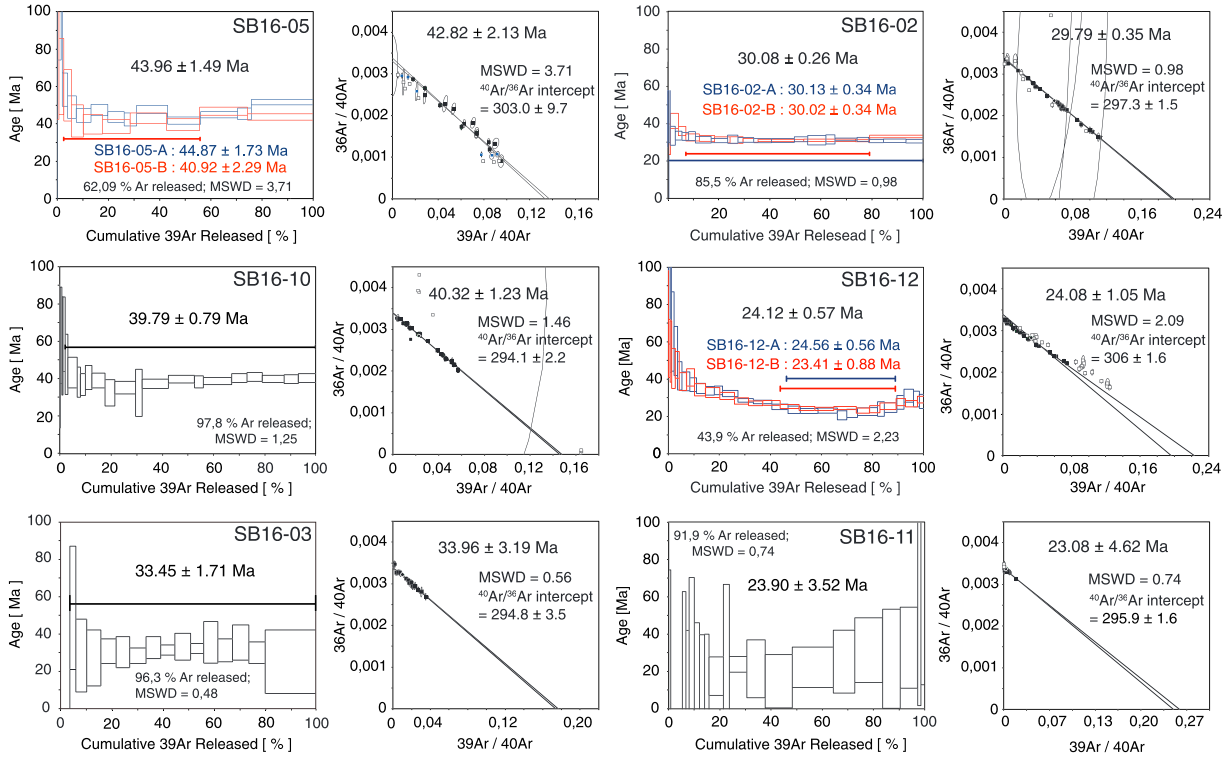

Figure 4. $^{40}Ar/^{39}Ar$ spectra and inverse isochron for the samples from St. Barthelemy. MSWD = mean square weighted deviation.

et al., 1979) that was discarded by Westercamp and Andreieff (1983a, 1983b). This result questions the previously proposed ages for the other andesitic lava flows (light pink, Figure 3) and some hyaloclastites (light green, Figure 3) occurring in this part of the island. The age of the final magmatic event, exemplified by volcanic pipes and associated breccia crosscutting the two dated lava flows (light yellow, Figure 3), may now be regarded as early Miocene at the oldest instead of early Oligocene; however, their age needs to be confirmed.

To sum up, our new results invalidate the overall chronology of the magmatism previously proposed by Westercamp and Andreieff (1983a, 1983b). We provide evidence for five (instead of three) main periods of magmatic activity: middle Eocene, late Eocene, early Oligocene, late Oligocene, and early Miocene. The magmatism of St. Barthelemy can no longer be considered as mainly middle Eocene in age. Instead, it spanned from middle Eocene to latest Oligocene-early Miocene times. These results also question the biostratigraphic determinations of the carbonate platform deposits that were mainly used to establish the previous chronology of the magmatic events (Westercamp & Andreieff, 1983a, 1983b). The same authors proposed that the deposition of all carbonate platforms took place in a <4-Ma period during the middle Eocene. Lastly, in the central-western and western part of the island, we dated dacitic lava flows at 33.45 ± 1.72 (sample SB16-03) and two andesitic lava flows at 23.90 ± 3.52 Ma and 24.31 ± 1.22 Ma (samples SB16-11 and SB16-12), respectively. The contacts of these lavas, previously mapped below the middle Eocene carbonate platform deposits, have been investigated again, and we show that the lava flowed in paleo-valleys that were carved into the carbonate platform deposit (Figure 3).

4.2. Deformation Pattern and Kinematics

4.2.1. Brittle Deformation

As mapped previously (Christman, 1953; Westercamp & Andreieff, 1983a, two main fault directions, N50°E and N140°E, and a minor direction of N90–110°E are identified. Irrespective of their trend, the fault planes show normal or transtensional kinematic indicators. At some places, N90°E trending faults are reverse with dm displacements (six locations across the island). However, we never observed two different kinematic indicators on the same fault plane, which means that we cannot propose a chronology. As a result, we define a chronology of deformations taking into account our new ages obtained on the magmatic rocks. In order to

Table 2
Main Faults: Results of the Paleostress Analysis Obtained From the Inversion of the Field Data

Sites	Longitude	Latitude	n/nt	σ_1	σ_2	σ_3	R′	α_w	QRw	QRt	Age of the deformed rock
1	−62.81725	17.91533	11/13	80/029	06/265	08/175	0.4	.02	C	C	Middle Eocene
2	−62.81583	17.91797	9/9	61/320	27/160	08/066	0.4	12.3	D	D	Middle Eocene
3	62.81 44	17.91 89	4/4	36/192	48/049	19/297	1.51	45.03	E	E	Middle Eocene
4	−62.81419	17.91758	2/2	73/087	08/329	15/237	0.5	11.65	E	E	Middle Eocene
5	−62.81200	17.91542	1/1	58/061	29/215	11/311	0.5	0	E	E	Middle Eocene
6	−62.81108	17.91525	1/1	58/302	30/140	08/045	0.5	0	E	E	Middle Eocene
7	−62.81256	17.88692	1/1	77/017	02/274	13/184	0.5	0	E	E	Early Oligocene
8	−62.81007	17.88468	3/3	67/134	04/235	23/326	0.67	60	E	E	Early Oligocene
9	−62.80306	17.90028	2/2	50/127	32/349	22/244	0.75	6.05	E	E	Early Oligocene
10	−62.80667	17.90222	5/7	55/093	32/248	12/346	0.6	—	E	E	Early Oligocene
11	−62.79722	17.90694	8/9	10/174	71/295	16/081	1.5	6.67	D	E	Early Oligocene
12	−62.79694	17.90778	10/14	85/15	01/120	05/210	0.9	4.34	C	D	Early Oligocene
13	−62.84014	17.89283	4/4	42/267	48/084	01/176	1.59	6.47	E	E	Early Oligocene
14	−62.83561	17.89325	7/7	36/132	43/264	26/021	1.41	2.56	D	D	Early Oligocene
15	−62.83131	17.88494	2/2	62/193	18/322	20/059	1.48	—	E	E	Early Oligocene
16	−62.80167	17.89472	22/27	14/092	76/279	02/182	1.51	3.55	C	D	Early Oligocene
17	−62.80333	17.89639	6/8	08/089	81/243	04/358	1.42	2.68	D	E	Early Oligocene
18	−62.79972	17.89639	4/4	24/051	52/286	27/154	0.5	—	E	E	Early Oligocene
19	−62.79444	17.90000	9/10	24/326	30/221	50/088	3	14.06	D	D	Early Oligocene
20	−62.79528	17.89944	3/3	72/152	10/273	16/006	0.48	—	E	E	Early Oligocene
21	−62.79283	17.90319	2/2	45/062	07/158	44/255	0.47	—	E	E	Early Oligocene
22	−62.79206	17.90149	3/3	33/162	56/326	07/067	0.33	—	E	E	Early Oligocene
23	−62.82762	17.88090	3/3	71/097	10/217	16/310	0.73	—	E	E	Early Oligocene
24	−62.84742	17.90400	17/21	31/275	56/067	13/177	0.78	10.14	B	D	Middle Miocene
25	−62.84739	17.90397	12/15	65/069	03/332	24/240	0.89	11.75	C	C	Middle Miocene
26	−62.85786	17.91300	2/2	59/214	18/092	25/354	0.5	22	E	E	Middle Miocene
27	−62.85889	17.91253	2/2	64/019	25/209	04/117	—	—	E	E	Middle Miocene
28	−62.85983	17.91100	5/7	07/006	24/273	65/111	2.27	7.68	E	E	Middle Miocene
29	−62.86181	17.90961	7/8	61/205	14/088	25/352	0.63	11.4	D	D	Middle Miocene
30	−62.85000	17.91000	4/5	69/268	01/174	21/084	0.22	5.55	E	E	Middle Miocene
31	−62.85556	17.91444	3/4	62/355	01/263	28/173	0.8	—	E	E	Middle Miocene
32	−62.85833	17.91222	12/15	50/126	21/008	32/264	0.09	9.49	C	C	Middle Miocene
33	−62.84389	17.91722	5/5	66/179	24/010	04/278	0.56	22.2	E	E	Middle Miocene
34	−62.86611	17.92361	6/7	66/310	24/129	00/219	0.61	3.35	D	D	Middle Miocene
36	−62.86694	17.92417	12/18	07/108	77/229	11/017	1.1	6.83	C	D	Middle Miocene

investigate the paleo stress field of St. Barthelemy during the middle Eocene to Oligocene-Miocene time span, we inverted the fault kinematics of 36 measurement sites for a total of 361 fault slip data (Table 2; Figures 5 and 6). At the outcrop scale, the inversions performed at each measurement site show that the faults are normal and show a dextral strike-slip to the SE and NW of the island whereas they show dextral strike-slip kinematics to the east (Figure 6). Based on our new chronology of the volcanic events, we performed grouped inversions on the faults that we estimate to have developed synchronously during the investigated time span.

4.2.1.1. Middle Eocene

The lowermost part of the series, middle Eocene in age, is affected by N50° and N140° trending faults. Syn-kinematic sedimentation is evidenced along the N140° trending faults as limestones deposited in the hanging wall of the fault show growth strata (Figure 5a). The paleostress inversion at each site reveals that both N140° and N50° trending faults display oblique slip (Table 1 and Figures 5a and 6a, sites 1 to 6). These structures are sealed by thick hyaloclastites in which a lava flow dated 40.92 ± 2.29 Ma is

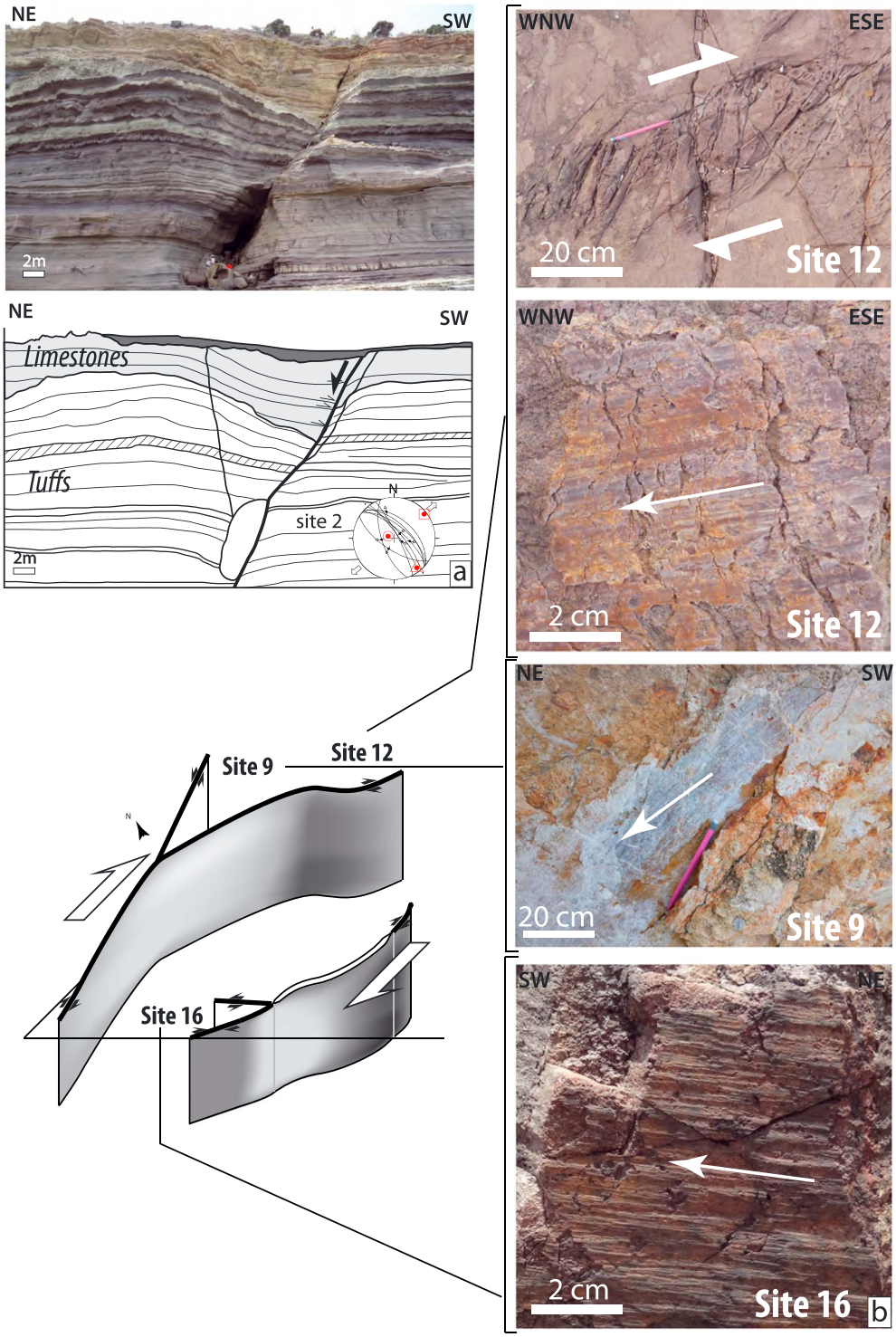

Figure 5. Field pictures showing brittle deformation examples from St. Barthelemy. (a) Synsedimentary faulting impacting the basement of the island. (b) Sketch and pictures illustrating the large-scale strike-slip system affecting the eastern tip of St. Barthelemy. The outcrop locations are provided in Figure 3, and the site locations are given in Figure 6.

intercalated (sample SB16-05; this study, see section 4.1). The paleostress tensor obtained from the field data for these rocks of middle Eocene age shows that σ_1 is almost vertical plunging 88° to the N147° trending fault, and σ_3 is horizontal and plunges N50°. The magnitude of σ_2 is close to σ_1 defining a pure extension regime with a principal direction of extension trending N50° (stereonet in Figure 6b, Table 3).

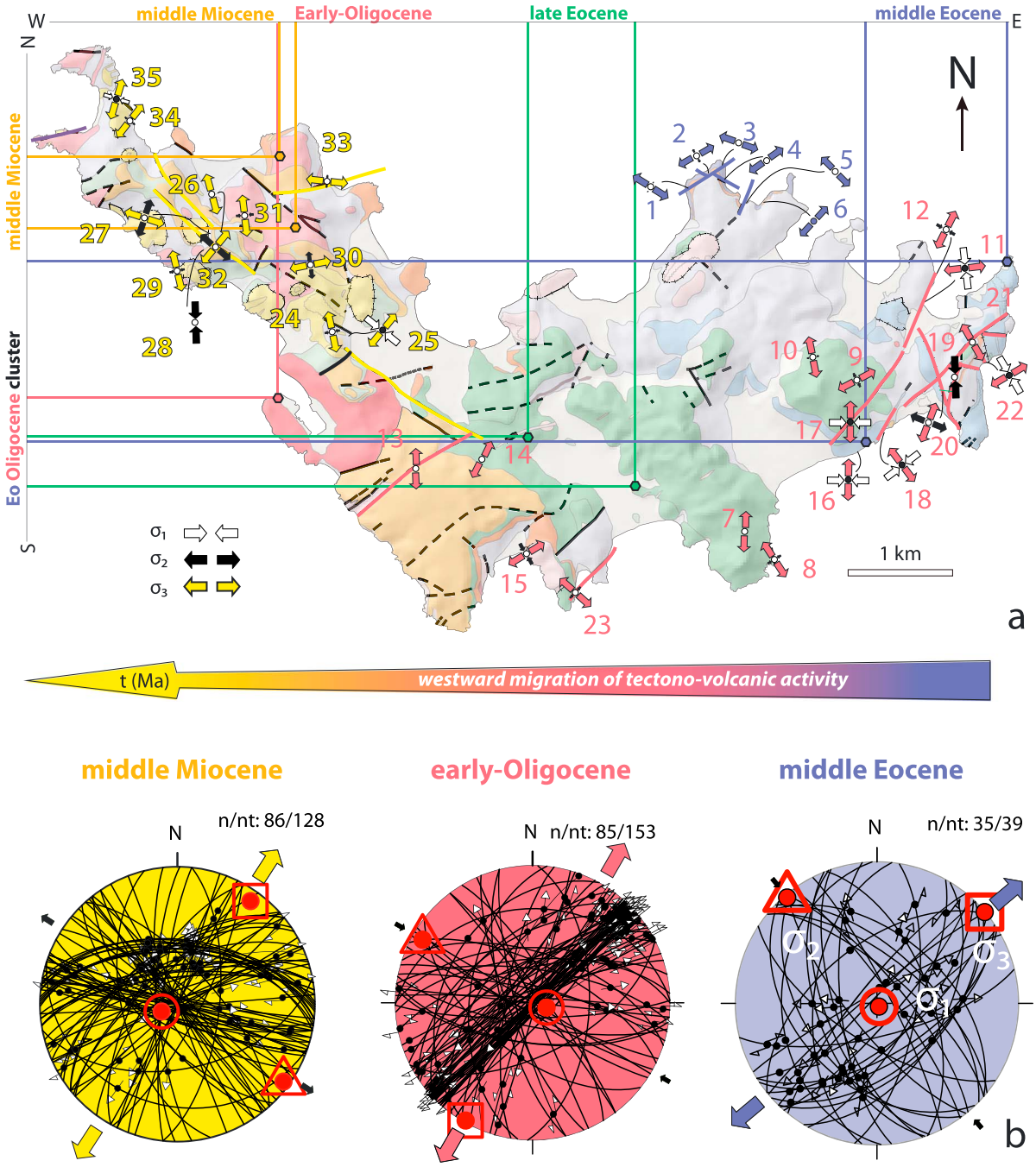

Figure 6. Results of the paleostress inversion in their tectono-magmatic context. (a) Schematic map of St. Barthelemy showing the westward migration of the tectono-magmatic activity and the paleostress tensor for each investigated fault on the island. The arrows show the azimuth of the horizontal stress axes with a length that is proportional to the stress magnitude. The outward and inward black arrows indicate compressive and extensive deviatoric stress axes, respectively (Delvaux et al., 1995). (b) Paleostress tensor obtained from the field data (faults with kinematic criteria, fractures, and dykes) for each of the three periods of volcanism identified in this study.

4.2.1.2. Early Oligocene

In the late Eocene, the magmatic units are mainly affected by N050° trending faults and are sometimes intruded by N50°E trending dykes. They mainly occur in the eastern-central part of the island and belong to the two oldest magmatic episodes. Consequently, the N50°E trending faults and dykes occurred after the late Eocene magmatic episode and we assumed that this deformation and associated dykes are

Table 3
The Paleostress Results Obtained From the Inversion of the Field Data for the Three Periods of Volcanism Identified in This Study

Chronology	n/nt	σ_1	σ_2	σ_3	R′	α_w	QRw	QRt
Middle Eocene	35/39	88/147	02/320	00/050	0.79	10.2	B	B
Early Oligocene	80/162	81/120	09/286	02/016	0.77	11.9	B	B
Middle Miocene	109/160	83/245	05/126	09/035	0.31	13.8	C	C

Oligocene in age. A dextral shear strain corridor that trends N050°E affects the eastern tip of the island (Figures 5b and 6a, sites 10 to 12 and 19 to 22). Southeast of the shear corridor, the N090°E trending faults are compressive (Figure 6a, site 19) and satellite shorter dextral strike-slip faults crop out (Figure 6a, sites 11 to 12 and 20 to 22). Northwest of the shear corridor, the N015°E and N120°E trending faults are sinistral (Figure 6, site 9) and dextral (Figure 6a, site 10) strike-slips, respectively. Faults showing trends ranging from N-S to N50°E display dip slip striae but without kinematics criteria (Figure 6a, site 10). These N50°E dextral strike-slip faults, which show pure strike-slip kinematics (subhorizontal striae), are intruded by dykes, most probably related to the early Oligocene magmatic event. Approaching the dykes, the slip on the fault becomes increasingly less oblique (striae plunging at 30°) allowing the magma to locally emplace along the fault. The paleostress tensor obtained from field data show that σ_3 is subhorizontal (−2°) and plunges N016°, and σ_2 is close to σ_1 defining a pure extension regime with a principal direction of extension trending N16° (stereonet Figure 6b; Table 3).

4.2.1.3. Middle Miocene

To the west of the island, the faults are crosscutting the magmatic bodies that intruded the lava flows we dated at ~24 Ma; therefore, their activity postdates the last early Miocene magmatic episode. As a result, we assumed that this tectonic episode is middle Miocene in age at the most; however, it could be younger. A series of large N110–140°E trending faults dissect the volcano-sedimentary pile (Figure 6a, Sites 26 to 41). The late Oligocene volcanic complex is bound to the south and north by E-W trending dextral strike-slip faults. It should be noted that the E-W trending faults, (Figure 6a, sites 36 and 40), are crosscut by NW-SE trending faults that show dip to oblique slip kinematics defining a N140°E trending dextral strike-slip corridor affecting the whole pile consisting of the youngest rocks we dated (west of the island). The paleostress tensor obtained from the field data show that σ_1 is almost vertical plunging 83° to the N245° fault, σ_3 is subhorizontal −9°- and trends N35°. σ_2 is extensional defining a radial extension regime with a N035° trending principal direction of extension (stereonet Figure 6b, Table 3).

5. Discussion

5.1. Tectono-Magmatic Evolution of St. Barthelemy

We show that the volcanism in St. Barthelemy spanned over the middle Eocene-early Miocene period with five main magmatic episodes. The structural analysis shows that the magmatism is associated with the deformation accommodated along the N050° and/or N140° trending faults. These two fault trends, N50° and N140° affect the base of the series, suggesting a strong interaction between the inherited N50° and N140° faults and the volcanism. Based upon the aforementioned magmatic evolution, three main tectonic events are identified.

The middle Eocene episode is characterized by a widespread submarine volcanism (and some intrusions) in the eastern part of the island of both tholeiitic and calc-alkaline affinity. At that time, a pure extension with a σ_3 directed N050° is accommodated along N110–140° trending faults. The two magmatic bodies dated in this study (central and eastern St. Barthelemy) most probably emplaced later along this structure. After a period of apparent volcanic quiescence, which may have lasted between 4 and 7 Ma, the calc-alkaline volcanism resumed during the late Eocene. Volcanic rocks of this age mainly outcrop in the central part of the island.

The early Oligocene magmatism is characterized by the large calc-alkaline intrusion occurring in the central-western part of the island (red-colored pluton, Figure 3), but some other small intrusions crosscutting the middle to late Eocene volcanics could also be attached to this magmatic episode (light red-colored intrusion, Figure 3). This magmatic episode occurred after a period of magmatic quiescence during which the large carbonate platform, outcropping in the central southern part of the island, developed.

The magmatic activity resumed during the late Oligocene with the eruption of arc-tholeiite lava flows. These lavas outcrop in the western part of the island where one of them (sample SB16-12) lay unconformably above the oldest mixed volcaniclastic-carbonate series. During the Oligocene, pure extension with a σ_3 directed N016° was accommodated along N120°E and 050°E trending faults. In the eastern part of the island, the intrusions show a N050°E trend suggesting that they could be Oligocene in age. Moreover, the magmatic bodies dated in this study show a N120°E elongation and were most probably emplaced along the N120°E fault (central and eastern St. Barthelemy). It should be noted that the dilation provided by the WinTensor program is larger along the N130°E trending fault than along the N050°E faults, which is fully consistent with the field observations of the larger intrusions trending N120°E and the smaller dykes intruded along the N050°E trending faults. Tilting along the N050°E trending and NW dipping faults may have been responsible for the general southeastward tilt of the series up to the late Oligocene. One of the consequences of this may have been the emersion of the northwestern part of the island. This is consistent with the unconformity observed between the late Oligocene lava flow and the underlying middle Eocene hyaloclatistes and suggests that the western part of the island was emerged and subjected to erosion prior to the late Oligocene.

The final magmatic event that mainly outcrops in the western part of the island is characterized by volcanic pipes and associated breccias crosscutting the late Oligocene lava flows. Some small intrusions occurring in the central and eastern parts of the island, even when they do not crosscut the late Oligocene lava flows, were supposedly related to this episode (Westercamp & Andreieff, 1983a, 1983b). However, we dated one of these intrusions (sample SB16-10) at 39.79 ± 0.78 Ma, which we therefore affiliate to a previous magmatic episode. Last, the radial extension with a N030° directed σ_3 that postdates the latest N110–140°E trending early Miocene lavas, was accommodated along the N110–140°E trending faults.

At the island scale, instead of a strict southward migration as previously proposed (Westercamp & Andreieff, 1983a, 1983b), we show that the magmatic activity migrated westward over the whole length of the island (tens of km) and shows an Eo-Oligocene cluster in the south and a northward migration during the late Oligocene-early Miocene (see the projection of our ages on the N-S and E-W axes, Figure 6). This result is in accordance with the regional westward migration of the Lesser Antilles arc volcanism that can be observed all along the arc, and in particular in its northeastern part where it is associated with a westward arc jump (Bouysses & Westercamp, 1990; Macdonald et al., 2000). This migration of the arc was thought to result from a slab flattening and break-off following the subduction of a buoyant ridge. This event was also believed to have triggered a compressive event and a magmatic gap between 30 and 20 Ma (Bouysses & Westercamp, 1990).

In this study we show that the arc was active in St. Barthelemy till early Miocene and that during the Eocene-Miocene time span the tectonic regime was extensive (pure or radial extension). This observation rules out (i) the hypothesis of a 10-Myr compressive event affecting the forearc of the Lesser Antilles during Oligocene and (ii) the westward arc migration between 30 and 20 Ma (Bouysses & Westercamp, 1990). Arc migration occurred thus later, that is, after early Miocene. Our results, suggest that the upper plate was undergoing regional extension contemporaneously with arc activity. We attribute this large-scale extension to reflect the accommodation by the upper Caribbean Plate of governed by large-scale plate kinematics (Boschman et al., 2014).

5.2. Links to the Regional Geodynamical Evolution

Although the time-space evolution of the magmatic arc activity can now be described precisely over the studied time period, the main directions of the paleostresses and the estimation of the bulk deformation accommodated by this area of the Lesser Antilles is still missing. Therefore, in order to discuss and picture the regional geodynamic evolution of the area, we restored its deformation based on available bathymetric, structural, seismic, and paleomagnetic data (Church & Allison, 2005; Jany, 1989; Jany et al., 1990; Laurencin et al., 2017; Reid et al., 1991). We identified and mapped the main faults segmenting the backarc, arc, and forearc domains given that they act as micro block boundaries, separating graben from horst. The available perpendicular and parallel-to-the-trench seismic lines of the basins bounding the Anguilla Bank -for which a rough chronostratigraphy is available (Jany, 1989; Jany et al., 1990)- allow us to account for the deformation accommodated in response to parallel and perpendicular-to-the-trench extension (Figure 7). Ultimately, by closing the basins and rotating the PRVI block by 25° in a clockwise direction in order to restore its 25° counterclockwise rotation (Reid et al., 1991), a two-step restoration is proposed (Figure 8).

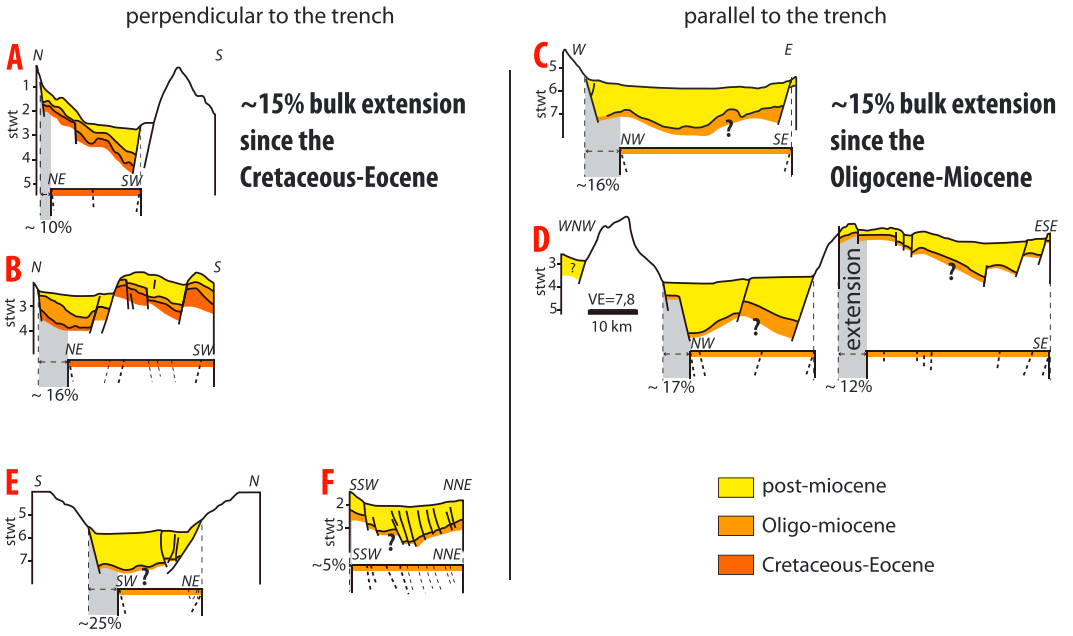

Figure 7. Seismic profiles interpreted by Jany (1989) and restored in this study, showing Cretaceous to Eocene infilling for profiles A and B in the Whiting Basin (to the west) and an eastward deepening of profiles C to F in these basins. As a result, the Cretaceous-Oligocene basement cannot be identified further eastward. The restorations show the bulk extension perpendicularly and parallel to the trench profiles over the Cretaceous-Miocene time period. All of the sections are drawn without vertical exageration except for section D. The locations of the profiles are provided in Figure 1b. sTWT signifies second Two-Way-Time.

Contemporaneously to the arc migration, the upper plate accommodated 12% of the perpendicular-to-the-trench extension in the basins located south of the PRVI block and west of the Anguilla Bank (cross-sections A, B and E, Figures 7 and 8a). In St. Barthelemy, the paleostress tensor estimated over the middle-Eocene shows a direction of extension that trends N050°E. Moreover, we show here that in St. Barthelemy, at least, the late Oligocene is a hinge period during which a switch from pure to radial extension accompanied the inland migration of the Lesser Antilles volcanic arc. This evolution reflects the introduction of a component of trench parallel extension and was followed by a Miocene dextral transtensive opening of the Anegada Trough (Jany et al., 1990; Laurencin et al., 2017) and the subsequent 25° counterclockwise rotation of the PRVI block (north of the Anegada Trough; Figure 8c). Our restoration with these boundary conditions gives a 15° clockwise rotation of the Anguilla Bank that should be tested further using paleomagnetic data, which are unfortunately not yet available south of the Anegada Trough. The evolution of the stress field pictured in St. Barthelemy seems to be significant at a regional scale and shows a σ1 tilt from a vertical to horizontal position resulting in a switch from pure to radial extension and ultimately dextral strike-slip. This evolution most probably reflects the initiation of strain partitioning in the upper Caribbean Plate. The high curvature of the trench (which has been acquired progressively through time) results in a northward increasing subduction obliquity that is accommodated in the upper Caribbean Plate by a sinistral strike-slip system made up of the E-W Enriquillo-Plantain Garden fault along the Greater Antilles and a N-S fault strike-slip fault along the Lesser Antilles volcanic arc; these two latter structures are parallel to the trench. The Anegada Trough accommodates differential motions onto these two large strike-slip faults. St. Barthelemy is located south of the trough and therefore provides evidence for the initiation of strain partitioning leading to the development of these large strike-slip faults within the upper Caribbean Plate (Figure 8c).

A last, younger volcanic episode (presently undated) has been described at the western tip of the island. Since the Oligocene, the basins located south of the PRVI block and in the Lesser Antilles backarc, such as the Kalinago Basin, have accommodated 15% of the parallel-to-the-trench extension (cross-sections C and D, Figure 7) while 15% of the perpendicular-to-the-trench extension was accommodated in the Kalinago Basin (cross-section F, Figures 7 and 8b). Therefore, the bulk extension was subequal along the parallel and

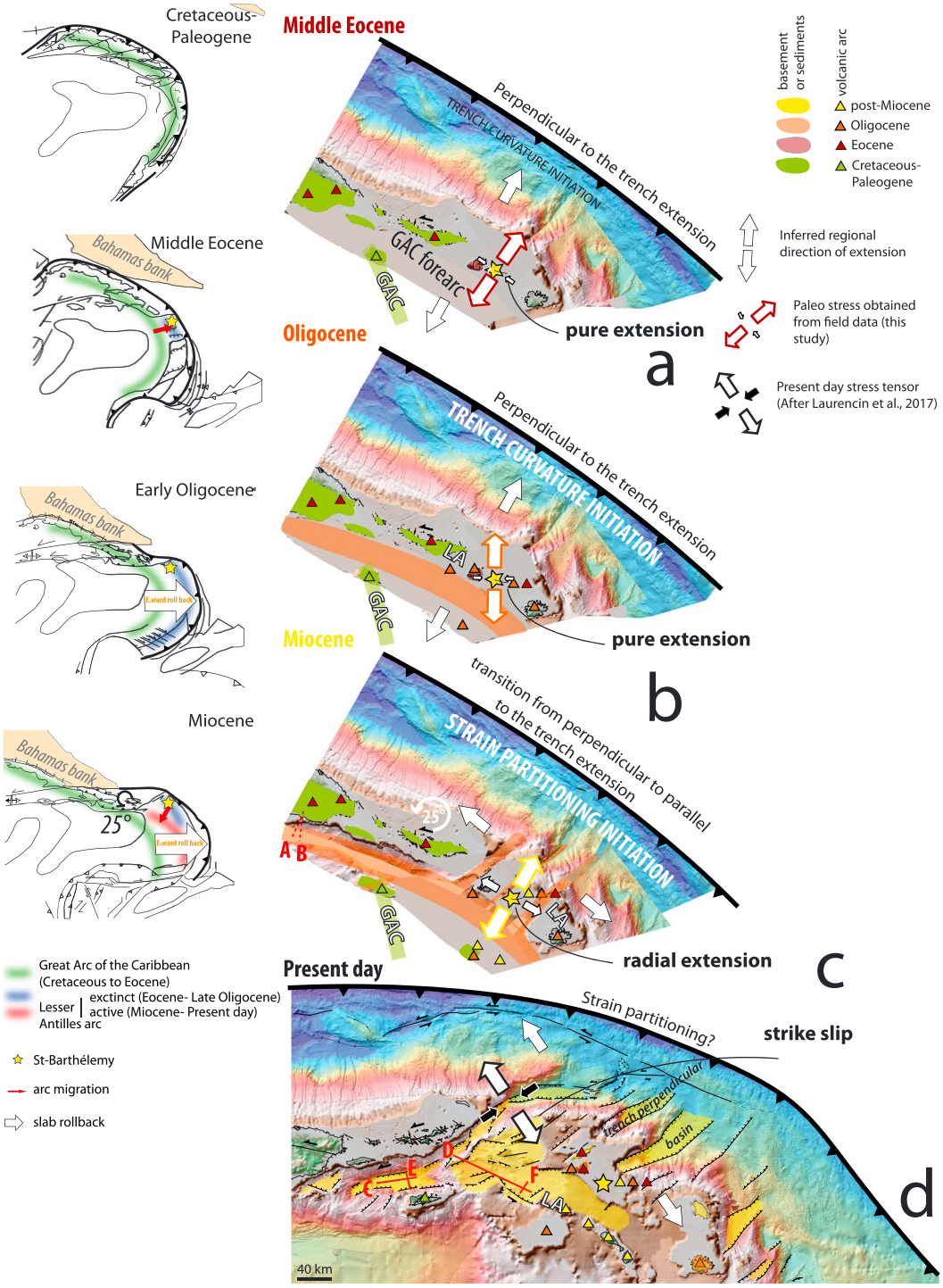

Figure 8. Three-step restoration of the Eocene to present-day geodynamical evolution of the PRVI block and Anguilla Bank. The background map used is a compilation of present-day bathymetric data from the Aguadomar cruise in 1999 (150-m resolution), the USGS marine cruises in 2002, 2003, 2006, and 2007 (Ten Brink et al., 2004), the Antithesis cruises in 2013 and 2016 (100-m resolution), and General Bathymetric Chart of the Oceans data (Becker et al., 2009; Smith & Sandwell, 1997; 300-m resolution). The left column shows the large-scale geodynamical evolution of the northeastern Caribbean Plate (after Pindell & Kennan, 2009). Traces of the main faults have been compiled based on the bathymetric map. Occurrences of outcrops of (i) the Cretaceous basement (Briggs & Akers, 1965; Church & Allison, 2005; Despretz et al., 1985; Monroe, 1980), (ii) the Eocene and Oligocene volcanism (Briden et al., 1979; Christman, 1953), and (iii) the Upper Miocene to active volcanism (Bouysse & Westercamp, 1990; Macdonald et al., 2000) are indicated by green, orange, and light orange colors, respectively. The timing of the opening of the basins is also provided (after Gill et al., 1989; Jany, 1989; Jany et al., 1990). The PRVI 25° counterclockwise rotation is taken from Reid et al. (1991). All of the paleogeographic maps are shown relative to a fixed North America (simplified from Pindell & Kennan, 2001, 2009 and Lao-Davila, 2014). GAC stands for the Great Arc of the Caribbean and LA stands for the Lesser Antilles arc.

perpendicular-to-the-trench cross section (restored cross section, Figure 7), which is somehow consistent with the Miocene radial extensional stress field obtained on St. Barthelemy. It should be noted that in sections C to F, the poor quality of seismic lines cannot be used to image the base of the series and we cannot rule out that the base of these basins consists of early-middle Eocene sediments, as observed on St. Martin and St. Barthelemy.

Last, a gap in the magmatism seems to have occurred between ~20 and ~10 Ma and was accompanied by an arc migration to its present-day position in the northeastern Lesser Antilles. As a result, the middle Eocene to early Miocene arc is now inactive and since then is found in the forearc of the present-day Lesser Antilles arc, which has been active since at least 10 Ma. This gap and westward migration of the volcanism were interpreted as being related to the subduction or a buoyant ridge of anomalous mid-Cretaceous crust (Bouysses & Westercamp, 1990).

At the scale of the whole Lesser Antilles, the tectono-magmatic evolution we describe here appears to be very similar to the one observed at the southern tip of the Lesser Antilles arc. In this region, the GAC magmatism migrated from the Aves Ridge to its forearc basin during middle Eocene times (c. 47 to c. 44 Ma) and ongoing calc-alkaline volcanism occurred until 38–33 Ma occurred on Las Testigos Island and in the neighboring Carúpano Basin (Speed & Smith-Horowitz, 1998, and references therein). The forearc basin of the GAC underwent flexural and then extensional regimes during the arc migration (Aitken et al., 2011). However, since the middle Eocene, the forearc underwent 70 km of bulk extension (37%) which is more than twice the one observed in the northeastern Lesser Antilles. The southern Lesser Antilles volcanic arc developed in an inverted forearc and led to the emergence, during the Miocene, of the present-day volcanic arc that divided the previously continuous Paleogene forearc basin into the present-day Grenada and Tobago Basins (Aitken et al., 2011). It must be pointed out that these basins had much higher subsidence (sediment thickness of ~12 km since the middle Eocene) than the basins developed in the northeastern Lesser Antilles. This is consistent with the fact that the bulk extension (and related subsidence) is much lower in the northern Lesser Antilles.

Regionally, the acceleration of the slab rollback and associated arc jump in the middle Eocene may have resulted from a narrowing of the subducting slab related to the GAC and/or from the collision at both the northern and southern tips of the GAC with the Bahamas Bank and South American continental crust, respectively (Aitken et al., 2011). The observed migration of the arc may also have been favored and enhanced by slab flattening due either to the entrance of the Bahamas Bank into the Greater Antilles subduction zone to the north or to the initiation of the slab tearing to the south (VanDecar et al., 2003). The difference in the bulk extension and subsidence in the forearc of the northeastern and southern Lesser Antilles may then reflect the differences in the slab geometry and behavior between the northern and southern ends of the subducting slab. To the north, the slab bends without tearing (Laurencin, 2017; van Benthem et al., 2013) thereby restraining the bulk extension of the upper plate whereas it is torn to the south allowing the upper plate to be more widely spread out (VanDecar et al., 2003).

5.3. Geodynamical insights

The collision of a buoyant anomaly in subduction zones is a common feature, and in this work we show that the analysis of the upper plate strain pattern of the subduction zone provides clues to the mechanical response of the overriding plate. The subduction of the laterally heterogeneous lithosphere bearing a buoyant anomaly results in a trench curvature as exemplified by the oroclinal bending of the Andes (Capitanio et al., 2011; Isacks, 1988) or other curved trenches such as the Hellenic, Papua New Guinea, Vanuatu, Tonga, Marianas and New Zealand trenches (Wallace et al., 2005, 2008). Wallace et al. (2005, 2008) proposed that the transitional zone between the subduction of the regular buoyancy material and the highly buoyant one exerts a torque force on the upper plate, which then triggers rapid microplate rotations possibly resulting in backarc rifting in some cases. St. Barthelemy and the whole Anguilla Bank are located above the type of transitional zone within the downgoing plate. The switch in the stress field recorded at the Oligo-Miocene hinge and the observed strain partitioning in the upper plate may be a direct expression of such torque force. Moreover, this study provides insight into the timing of the mechanical response of the crust during a regional stress change. We show that the switch from pure to radial extension and then strike-slip occurred over 10 Myr approximately. This switch indicates a peculiar evolution of the stress field during which σ_1 is progressively tilting from a vertical to a horizontal position.

6. Conclusions

Our integrative field study of St. Barthelemy Island combines geochronology, sedimentology, and structural data with paleostress inversions and enables us to

1. propose a revised timing for the volcanic arc activity in this region of the Antilles as we show that it was active from the middle-Eocene to the early Miocene;
2. show a westward migration of the tectono-volcanic activity on St. Barthelemy, comparable to the one observed on the other volcanic islands of the Lesser Antilles, which was mostly related to the Lesser Antilles arc activity rather than to Greater Arc of the Caribbean as previously suggested;
3. show a switch in the stress field from pure to radial extension over the middle Eocene-middle Miocene time span that corresponds to progressive trench bending and the initiation of the strain partitioning in the Caribbean upper plate.

These local observations made on St. Barthelemy also provide insights at a regional scale, such as

1. the arc activity in the region that was previously the forearc of the Great Arc of the Caribbean lasted until the early Miocene;
2. the switch in the stress field at the Oligo-Miocene hinge indicates the initiation of the strain partitioning in the upper Caribbean Plate, which occurred in response to trench bending following the entrance of the Bahamas Bank into the subduction zone;
3. we show that the northern end of the Lesser Antilles arc has a similar tectono-volcanic evolution as the southern one;
4. the north-south dichotomy in the perpendicular-to-the-trench extension, 15% in the north versus 30% in the south reflects slab ends that are highly curved to the north (limiting the amount of extension in the upper plate) and slab tear to the south (allowing for a large-scale extension of the upper plate).

Acknowledgments
Financial support was provided by the GEOTREF project (ADEME-AMI-GDG), INSU TelluS-SYSTER grant call 2017 and GAARAnti project (ANR-17-CE31-0009). Data have been deposited in the AGU repository. We would like to thank Ben Maunder for his review and suggestions that greatly improved our manuscript as well as Jeroen van Huenen for his editorial work. The authors thank S. Mullin for her corrections of their nonnative English. We warmly thank the researchers from the GEOTREF consortium for fruitful discussions during the fieldwork campaigns in Guadeloupe and during scientific meetings. St. Barthelemy COM is thanked for housing us in Plaine des Jeux. Hélène, Odile, Brigitte, and St Barth Essentiel are also thanked for their kindness and help during the fieldwork. All the data used are listed in the references or archived in https://drive.google.com/open?id=1aIJPqn1cNrnbLYFGq7hfRdt7fZs3QQUM repository.

References

Aitken, T., Mann, P., Escalona, A., & Christeson, G. L. (2011). Evolution of the Grenada and Tobago basins and implications for arc migration. *Marine and Petroleum Geology*, *28*(1), 235–258.

Andreieff, P., Bouysse, P., & Westercamp, D. (1987). Géologie de l'arc insulaire des Petites Antilles, et évolution géodynamique de l'Est-Caraïbe, Thèse de Doctorat d'état, Université de Bordeaux I.

Angelier, J. (1979). Determination of the mean principal directions of stresses for a given fault population. *Tectonophysics*, *56*(7), 17–26.

Angelier, J., & Mechler, P. (1977). Sur une méthode graphique de recherche des contraintes principales également utilisable en tectonique et en séismologie: La méthode des dièdres droits. *Bulletin de la Société Géologique de France*, *7*(XIX n°6), 1309–1318.

Barker, P. F. (1970). Plate tectonics of the Scotia Sea region. *Nature*, *228*(5278), 1293–1296. https://doi.org/10.1038/2281293a0

Becker, J. J., Sandwell, D. T., Smith, W. H. F., Braud, J., Binder, B., Depner, J., et al. (2009). Global bathymetry and elevation data at 30 arc seconds resolution: SRTM30_PLUS. *Marine Geodesy*, *32*(4), 355–371.

Bonneton, J. R., & Vila, J. M. (1983). Donnees geologiques nouvelles a l9lle de Saint-Martin (Petites Antilles). *Bulletin de la Société Géologique de France*, *7*(6), 867–871.

Boschman, L. M., van Hinsbergen, D. J., Torsvik, T. H., Spakman, W., & Pindell, J. L. (2014). Kinematic reconstruction of the Caribbean region since the Early Jurassic. *Earth-Science Reviews*, *138*, 102–136.

Bouysse, P., Andreieff, P., Richard, M., Baudron, J., Mascle, A., Maury, R., & Westercamp, D. (1985). Aves swell and northern Lesser Antilles rodge: Rock-dredging results from ARCANTE 3 cruise. In A. Mascle (Ed.), *Caribbean geodynamics* (pp. 65–76). Paris: Editions Technip.

Bouysse, P., Westercamp, D., & Andreieff, P. (1990). The Lesser Antilles island arc. *Proceedings. Ocean Drilling Program. Scientific Results*, *110*, 29–44.

Bouysses, P., & Westercamp, D. (1990). Subduction of Atlantic aseismic ridges and Late Cenozoic evolution of the Lesser Antilles island arc. *Tectonophysics*, *175*, 349–380.

Briden, J. C., Rex, D. C., Faller, A. M., & Tomblin, J. F. (1979). K-Ar geochronology and palaeomagnetism of volcanic rocks in the Lesser Antilles island arc. *Philosophical transactions of the Royal Society A: Mathematical, Physical and Engineering Sciences*, *291*(1383), 485–528. https://doi.org/10.1098/rsta.1979.0040

Briggs, R., & Akers, J. (1965). Hydrogeologic map of Puerto Rico and adjacent islands.

Capitanio, F. A., Faccenna, C., Zlotnik, S., & Stegman, D. R. (2011). Subduction dynamics and the origin of Andean orogeny and the Bolivian orocline. *Nature*, *480*(7375), 83. https://doi.org/10.1038/nature10596

Christman, R. A. (1953). Geology of St. Bartholomew, St. Martin, and Anguilla, Lesser Antilles. *Bulletin Geological Society of America*, *64*(1), 65–96. https://doi.org/10.1130/0016-7606(1953)64%5B85:GOSBSM%5D2.0.CO;2

Church, R. E., & Allison, K. R. (2005). The petroleum potential of the Saba Bank Area, Netherlands Antilles. *First Break*, *23*(2), 71–76. https://doi.org/10.1007/978-3-642-79476-6_14

Corsini, M., Lardeaux, J. M., Verati, C., Voitus, E., & Balagne, M. (2011). Discovery of lower cretaceous synmetamorphic thrust tectonics in French Lesser Antilles (La Desirade Island, Guadeloupe): Implications for Caribbean geodynamics. *Tectonics*, *30*, TC4005. https://doi.org/10.1029/2011TC002875

De Min, L., Lebrun, J. F., Cornée, J. J., Münch, P., Léticée, J. L., Quillévéré, F., et al. (2015). Tectonic and sedimentary architecture of the Karukéra spur: A record of the Lesser Antilles fore-arc deformations since the Neogene. *Marine Geology*, *363*, 15–37. https://doi.org/10.1016/j.margeo.2015.02.007

De Reynal de Saint-Michel (1966). Saint-Barthélemy Cartes et croquis,
Delvaux, D., Moeys, R., Stapel, G., Melnikov, A., & Ermikov, V. (1995). Paleostress reconstruction and geodynamics of the Baikal region, Central Asia. Part I. Pre-rift evolution: Paleozoic and Mesozoic. *Tectonophysics*, *252*, 61–101.
Delvaux, D., & Sperner, B. (2003). New aspects of tectonic stress inversion with reference to the TENSOR program. *Geological Society of London, Special Publication*, *212*(1), 75–100. https://doi.org/10.1144/GSL.SP.2003.212.01.06
DeMets, C., Jansma, P. E., Mattioli, G. S., Dixon, T. H., Farina, F., Bilham, R., et al. (2000). GPS geodetic constraints on Caribbean-North America plate motion. *Geophysical Research Letters*, *27*(3), 437–440. https://doi.org/10.1029/1999GL005436
Deng, J., & Sykes, L. R. (1995). Determination of Euler pole for contemporary relative motion of Caribbean and North American plates using slip vectors of interplate earthquakes. *Tectonics*, *14*(1), 39–53. https://doi.org/10.1029/94TC02547
Despretz, J. M., Daly, T. E., & Robinson, E. (1985). Geology and petroleum potential of Saba Bank area, northeastern Caribbean. *AAPG Bulletin*, *69*(2), 249–249.
England, P., Engdahl, R., & Thatcher, W. (2004). Systematic variation in the depths of slabs beneath arc volcanoes. *Geophysical Journal International*, *156*(2), 377–408. https://doi.org/10.1111/j.1365-246X.2003.02132.x
Escalona, A., & Mann, P. (2010). Tectonics, basin subsidence mechanisms, and paleogeography of the Caribbean-South American plate boundary zone. *Marine and Petroleum Geology*, *28*, 8–39. https://doi.org/10.1016/j.marpetgeo.2010.01.016
Feuillet, N., Beauducel, F., & Tapponnier, P. (2011). Tectonic context of moderate to large historical earthquakes in the Lesser Antilles and mechanical coupling with volcanoes. *Journal of Geophysical Research*, *116*, B10308. https://doi.org/10.1029/2011JB008443
Feuillet, N., Leclerc, F., Tapponnier, P., Beauducel, F., Boudon, G., Le Friant, A., et al. (2010). Active faulting induced by slip partitioning in Montserrat and link with volcanic activity: New insights from the 2009 GWADASEIS marine cruise data. *Geophysical Research Letters*, *37*, L00E15. https://doi.org/10.1029/2010GL042556
Feuillet, N., Manighetti, I., & Tapponnier, P. (2001). Extension active perpendiculaire à la subduction dans l'arc des Petites Antilles (Guadeloupe, Antilles françaises). *Comptes Rendus de l'Académie des Sciences - Series IIA - Earth and Planetary Science*, *333*(9), 583–590.
Feuillet, N., Manighetti, I., Tapponnier, P., & Jacques, E. (2002). Arc parallel extension and localization of volcanic complexes in Guadeloupe, Lesser Antilles. *Journal of Geophysical Research*, *107*(B12), 2331. https://doi.org/10.1029/2001JB000308
Fox, P. J., Schreiber, E., & Heezen, B. C. (1971). The geology of the Caribbean crust: Tertiary sediments, granitic and basic rocks from the Aves Ridge. *Tectonophysics*, *12*(2), 89–109.
Germa, A., Quidelleur, X., Labanieh, S., Chauvel, C., & Lahitte, P. (2011). The volcanic evolution of Martinique Island: Insights from K–Ar dating into the Lesser Antilles arc migration since the Oligocene. *Journal of Volcanology and Geothermal Research*, *208*(3), 122–135.
Gill, I. P., Hubbard, D. K., Maclaughlin, P., & Moore, C. H. (1989). Sedimentological and tectonic evolution of Tertiary St. Croix. In D. K. Hubbard (Ed.), *12th Caribbean Geological Conference* (pp. 49–71).
Gonzàlez, O.'. L., Clouard, V., & Zahradnik, J. (2017). Moment tensor solutions along the central Lesser Antilles using regional broadband stations. *Tectonophysics*, *717*, 217–225.
Heuret, A., & Lallemand, S. (2005). Plate motions, slab dynamics and back-arc deformation. *Physics of the Earth and Planetary Interiors*, *149*, 31–51. https://doi.org/10.1016/j.pepi.2004.08.022
Isacks, B. L. (1988). Uplift of the Central Andean Plateau and bending of the Bolivian Orocline. *Journal of Geophysical Research*, *93*(B4), 3211–3231.
Jansma, P. E., Mattioli, G. S., Lopez, A., DeMets, C., Dixon, T. H., Mann, P., & Calais, E. (2000). Neotectonics of Puerto Rico and the Virgin Islands, northeastern Caribbean, from GPS geodesy. *Tectonics*, *19*(6), 1021–1037.
Jany, I. (1989). Neotectonique au sud des grandes antilles: Collision (ride de beata, presqu'ile de bahoruco): Subduction (fosse de los muertos), transtension (passage d'anegada).
Jany, I., Scanlon, K. M., & Mauffret, A. (1990). Geological interpretation of combined Seabeam, Gloria and seismic data from Anegada Passage (Virgin Islands, north Caribbean). *Marine Geophysical Researches*, *12*(3), 173–196. https://doi.org/10.1007/BF02266712
Koppers, A. A. (2002). ArArCALC—Software for 40 Ar/39 Ar age calculations. *Computers & Geosciences*, *28*(5), 605–619.
Ladd, J. W., & Sheridan, R. E. (1987). Seismic stratigraphy of the Bahamas. *American Association of Petroleum Geologists Bulletin*, *71*(6), 719–736.
Lallemand, S. (1999). *La subduction océanique*. Gordon & Breach, Paris.
Lao-Davila, D. A. (2014). Collisional zones in Puerto Rico and the northern Caribbean. *Journal of South American Earth Sciences*, *54*, 1–19. https://doi.org/10.1016/j.jsames.2014.04.009
Lardeaux, J. M., Munch, P., Corsini, M., Cornee, J. J., Verati, C., Lebrun, J. F., et al. (2013). La Désirade island (Guadeloupe, French West Indies): A key target for deciphering the role of reactivated tectonic structures in Lesser Antilles arc building. *Bulletin de la Societe Geologique de France*, *184*(1–2), 21–34. https://doi.org/10.2113/gssgfbull.184.1-2.21.
Laurencin, M. (2017). Etude de la structure profonde du passage d'Anegada et de la zone de subduction des Iles Virges: Déformation tectonique et simogénèse. PhD Thesis, 294 p. UBO Brest.
Laurencin, M., Marcaillou, B., Graindorge, D., Klingelhoefer, F., Lallemand, S., Laigle, M., & Lebrun, J.-F. (2017). The polyphased tectonic evolution of the Anegada Passage in the northern Lesser Antilles subduction zone. *Tectonics*, *36*, 945–961. https://doi.org/10.1002/2017TC004511
Lopez, A. M., Stein, S., Dixon, T., Sella, G., Calais, E., Jansma, P., et al. (2006). Is there a northern Lesser Antilles forearc block? *Geophysical Research Letters*, *33*, L07313. https://doi.org/10.1029/2005GL025293
Lynner, C., & Long, M. D. (2013). Sub-slab seismic anisotropy and mantle flow beneath the Caribbean and Scotia subduction zones: Effects of slab morphology and kinematics. *Earth and Planetary Science Letters*, *361*, 367–378. https://doi.org/10.1016/j.epsl.2012.11.007.
Macdonald, R., Hawkesworth, C. J., & Heath, E. (2000). The Lesser Antilles volcanic chain: A study in arc magmatism. *Earth-Science Reviews*, *49*(1), 1–76.
Manaker, D. M., Calais, E., Freed, A. M., Ali, S. T., Przybylski, P., Mattioli, G., et al. (2008). Interseismic plate coupling and strain partitioning in the northeastern Caribbean. *Geophysical Journal International*, *174*(3), 889–903.
Mann, P. (1999). Caribbean sedimentary basins: Classification and tectonic setting from Jurassic to present. *Sedimentary Basins of the World*, *4*, 3–31.
Mann, P. (2012). Comparison of structural styles and giant hydrocarbon occurrences within four active strike-slip regions: California, Southern Caribbean, Sumatra, and East China.
Mann, P., Hippolyte, J.-C., Grindlay, N. R., & Abrams, L. J. (2005). Neotectonics of southern Puerto Rico and its offshore margin. *Geological Society of America Special Papers*, *385*, 173–214.
Monroe, W. H. (1980). Geology of the middle Tertiary formations of Puerto Rico, US Govt. Print. Off, 953.
Münch, P., Cornee, J. J., Lebrun, J. F., Quillevere, F., Verati, C., Melinte-Dobrinescu, M., et al. (2014). Pliocene to Pleistocene vertical movements in the forearc of the Lesser Antilles subduction: Insights from chronostratigraphy of shallow-water carbonate platforms (Guadeloupe archipelago). *Journal of the Geological Society*, *171*(3), 329–341.

Nagle, F., Stipp, J. J., & Fisher, D. E. (1976). K-Ar geochronology of the limestone caribbees and Martinique, lesser Antilles, West Indies. *Earth and Planetary Science Letters*, *29*, 401–412.

Neill, I., Kerr, A. C., Hastie, A. R., Stanek, K. P., & Millar, I. L. (2011). Origin of the Aves Ridge and Dutch–Venezuelan Antilles: Interaction of the Cretaceous 'Great Arc'and Caribbean–Colombian Oceanic Plateau? *Journal of the Geological Society*, *168*(2), 333–348.

Pindell, J., & Kennan, L. (2001). Kinematic evolution of the Gulf of Mexico, Pet. Syst. Deep. Basins, GCSSEPM Found. 21st Annu. Bob F. Perkins Res. Conf., 193–220. https://doi.org/10.5724/gcs.01.21.0159

Pindell, J., Maresch, W. V., Martens, U., & Stanek, K. (2012). The Greater Antillean Arc: Early Cretaceous origin and proposed relationship to Central American subduction mélanges: Implications for models of Caribbean evolution. *International Geology Review*, *54*(2), 131–143. https://doi.org/10.1080/00206814.2010.510008

Pindell, J. L., & Barrett, S. F. (1990). Geological evolution of the Caribbean region: A plate tectonic perspective, Caribb. Reg. Boulder, Color. Geol. Soc. Am. Geol. North Am., H(405–432).

Pindell, J. L., & Kennan, L. (2009). Tectonic evolution of the Gulf of Mexico, Caribbean and northern South America in the mantle reference frame: An update. *Origin and Evolution of the Caribbean Plate*, *328*(1), 1–55. https://doi.org/10.1144/sp328.1

Reid, A., Plumley, W., & Schellekens, J. H. (1991). Paleomagnetic evidence for late miocene counterclockwise rotation of north coast carbonate sequence, Puerto Rico. *Geophysical Research Letters*, *18*(3), 565–568. https://doi.org/10.1029/91GL00401

Renne, P. R., Mundil, R., Balco, G., Min, K., & Ludwig, K. R. (2010). Joint determination of 40K decay constants and 40Ar*/40K for the Fish Canyon sanidine standard, and improved accuracy for 40Ar/39Ar geochronology. *Geochimica et Cosmochimica Acta*, *74*, 5349–5367. https://doi.org/10.1016/j.gca.2010.06.017

Smith, W. H., & Sandwell, D. T. (1997). Global sea floor topography from satellite altimetry and ship depth soundings. *Science*, *277*(5334), 1956–1962.

Speed, R. C., Gerhard, L. C., & McKee, E. H. (1979). Ages of deposition, deformation, and intrusion of Cretaceous rocks, eastern St. Croix, Virgin Islands. *Geological Society of America Bulletin Part I*, *90*, 629–632.

Speed, R. C., & Smith-Horowitz, P. L. (1998). The Tobago Terrane. *International Geology Review*, *40*(9), 805–830.

Stein, S., Engeln, J. F., Wiens, D. A., Fujita, K., & Speed, R. C. (1982). Subduction Seismicity and Tectonics in the Lesser Antilles Arc. *Journal of Geophysical Research*, *87*(B10), 8642–8664. https://doi.org/10.1029/JB087iB10p08642

Symithe, S., Calais, E., De Chabalier, J. B., Robertson, R., & Higgins, M. (2015). Current block motions and strain accumulation on active faults in the Caribbean. *Journal of Geophysical Research: Solid Earth*, *120*, 3748–3774. https://doi.org/10.1002/2014JB011779

Syracuse, E. M., & Abers, G. A. (2006). Global compilation of variations in slab depth beneath arc volcanoes and implications. *Geochemistry, Geophysics, Geosystems*, *7*, Q05017. https://doi.org/10.1029/2005GC001045

Tatsumi, Y., Hamilton, D. L., & Nesbitt, R. W. (1986). Chemical characteristics of fluid phase released from a subducted lithosphere and origin of arc magmas: Evidence from high-pressure experiments and natural rocks. *Journal of Volcanology and Geothermal Research*, *29*(1–4), 293–309.

Ten Brink, U., & Lin, J. (2004). Stress interaction between subduction earthquakes and forearc strike-slip faults: Modeling and application to the northern Caribbean plate boundary. *Journal of Geophysical Research*, *109*, B12310. https://doi.org/10.1029/2004JB003031

Uchupi, E., Milliman, J., Luyendyk, B., Bowin, C., & Emery, K. (1971). Structure and origin of Southeastern Bahamas. *American Association of Petroleum Geologists*, *55*(5), 687–704.

van Benthem, S., Govers, R., Spakman, W., & Wortel, R. (2013). Tectonic evolution and mantle structure of the Caribbean. *Journal of Geophysical Research: Solid Earth*, *118*, 3019–3036. https://doi.org/10.1002/jgrb.50235

VanDecar, J. C., Russo, R. M., James, D. E., Ambeh, W. B., & Franke, M. (2003). Aseismic continuation of the Lesser Antilles slab beneath continental South America. *Journal of Geophysical Research*, *108*(B1), 2043. https://doi.org/10.1029/2001JB000884

Vandenberghe, N., Hilgen, F., & Speijer, R. (2012). The Paleogene period. In F. Gradstein, et al. (Eds.), *The geologic time scale 2012* (pp. 855–922). Amsterdam: Elsevier. https://doi.org/10.1016/B978-0-444-59425-9.00028-7

Wallace, L. M., Ellis, S., & Mann, P. (2008). *Tectonic block rotation, arc curvature, and back-arc rifting: Insights into these processes in the Mediterranean and the western Pacific*, *IOP Conference Series: Earth and Environmental Science* (Vol. 2, 012010). University of Texas at Austin, Jackson School of Geosciences, USA.

Wallace, L. M., McCaffrey, R., Beavan, J., & Ellis, S. (2005). Rapid microplate rotations and backarc rifting at the transition between collision and subduction. *Geology*, *33*(11), 857–860.

Westbrook, G. K., & McCann, W. R. (1986). Subduction of Atlantic lithosphere beneath the Caribbean. *Geology of North American*, *1000*, 341–350.

Westercamp, D., & Andreieff, P. (1983a). Carte géologique de Saint-Barthélemy et ses îles à 1/20 000.

Westercamp, D., & Andreieff, P. (1983b). Saint-Barthélemy et ses îles, Antilles françaises: Stratigraphie et évolution magmato-structurale. *Bulletin de la Société Géologique de France*, *XXV*(n°6), 873–883.